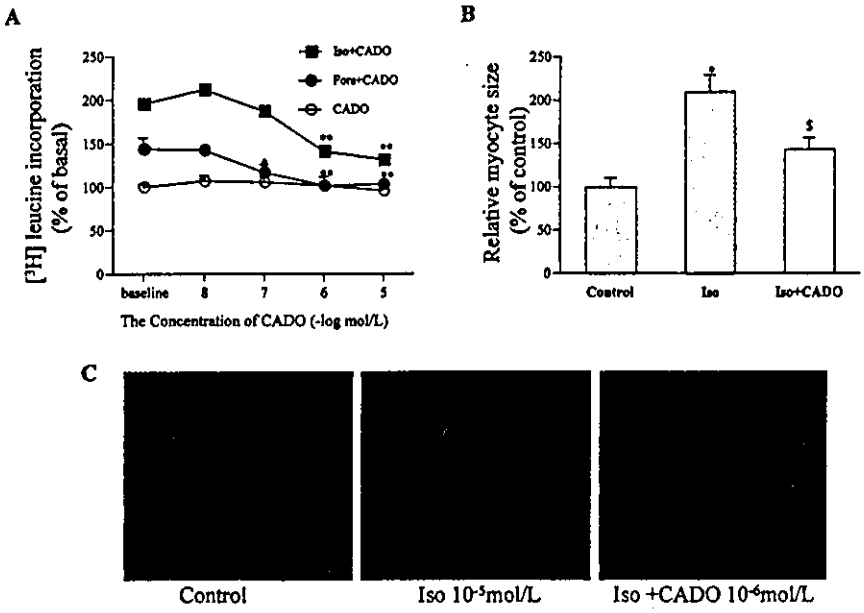

Figure 2. Inhibitory effects of CADO on protein synthesis stimulated by Iso (10^{-5} mol/L) or forskolin (Fors, 10^{-5} mol/L). A, Concentration-dependent effects of CADO on [^{3}H]leucine incorporation induced by Iso or Fors. *P<0.05, **P<0.01 compared with the value at baseline. B, Enlargement of myocyte cross-sectional area induced by Iso (10^{-5} mol/L) was decreased in the presence of CADO (10^{-6} mol/L), *P<0.01 compared with the value at control, $$P$<0.01 vs PE (n=200 cells in every group). C, Representative confocal microscopic images of myocytes with rhodamine-phalloidin staining of actin and DAPI staining of the nucleus. Values are expressed as mean±SEM. Every experiment was repeated at least 3 times.

results may be attributed to the use of minipump to deliver the drugs in a stable and low concentration that did not significantly affect hemodynamics and also suggest that the antihypertrophic effect of CADO is independent of blood pressure change. The trans-stenosis pressure gradients were similar in all the mice that received TAC treatment. The results of hemodynamics at 4 weeks are shown in the Table.

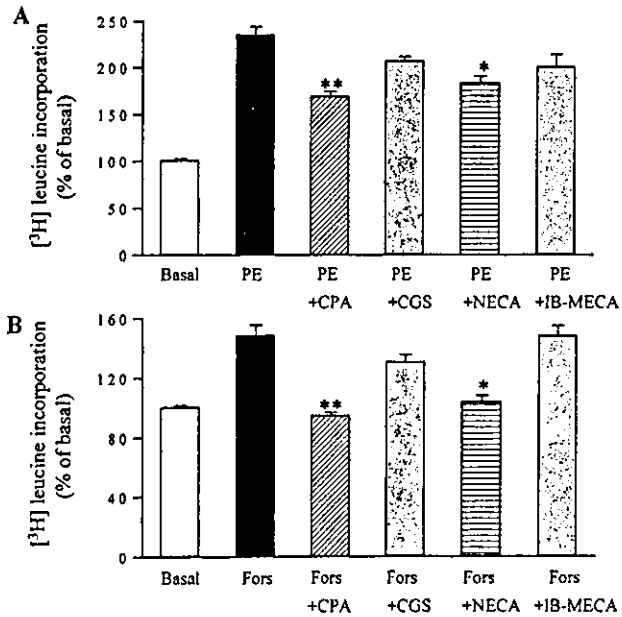

Figure 3. Effects of adenosine receptor agonists on myocyte hypertrophy induced by PE (A) or forskolin (B). Values are expressed as mean±SEM, *P<0.05, **P<0.01 compared with PE or forskolin alone. Every experiment was repeated at least 3 times. Concentration of PE and forskolin was 10^{-4} and 10^{-5} mol/L, respectively; concentration of other agents is 10^{-6} mol/L; CGS indicates 2-*p*-(2-carboxyethyl) phenethylamino-5′-*N*-ethylcarboxamino adenosine hydrochloride.

Activation of Adenosine A_1 Receptors Prevents Heart Failure In Vivo

Pressure overload induced CHF manifested by increases in the lung weight and reduction in fractional shortening (FS) and LV dP/dt_{max}. In TAC mice, the lung weight to body weight ratio increased by an average of 93%, the treatment with CADO markedly ameliorated pulmonary congestion by ≈80%, and even no significant difference was found on the lung weight to body weight ratio between CADO-treated TAC mice and sham-operated mice (Figures 6A and 6B). Comparable results are also observed in CPA-treated TAC mice (Figure 6A). We defined lung weight to body weight ratio higher than mean±4 SD in sham mice as the criteria for pulmonary congestion; consequently, the incidence of pulmonary congestion was 62% (16 of 29) in saline-treated TAC mice, which is dramatically higher relative to 15% (3 of 20) in CADO-treated TAC mice (P=0.0013). FS and LV dP/dt_{max} also increased in either CADO- or CPA-treated mice compared with saline-treated TAC mice (Figures 6C and 6D). Linear correlation analysis noted a significant positive correlation between the heart weight to body weight ratio and the lung weight to body weight ratio (r=0.857, P<0.001).

Discussion

In this study we were able to demonstrate for the first time that the stimulation of adenosine receptors can effectively attenuate myocyte hypertrophy in vitro and in vivo and improve functioning of the pressure-overloaded heart. Our findings also suggest that these beneficial effects on cardiac hypertrophy and heart function are mediated by adenosine A_1 receptors.

As shown in this study, the stimulation of adenosine receptors attenuated G-protein–coupled receptor–induced cardiac hypertrophy in vitro, which suggests that adenosine receptor–induced intracellular signaling may interfere with the cardiac hypertrophic signaling. To clarify this issue, we examined what type of adenosine receptors is involved in this

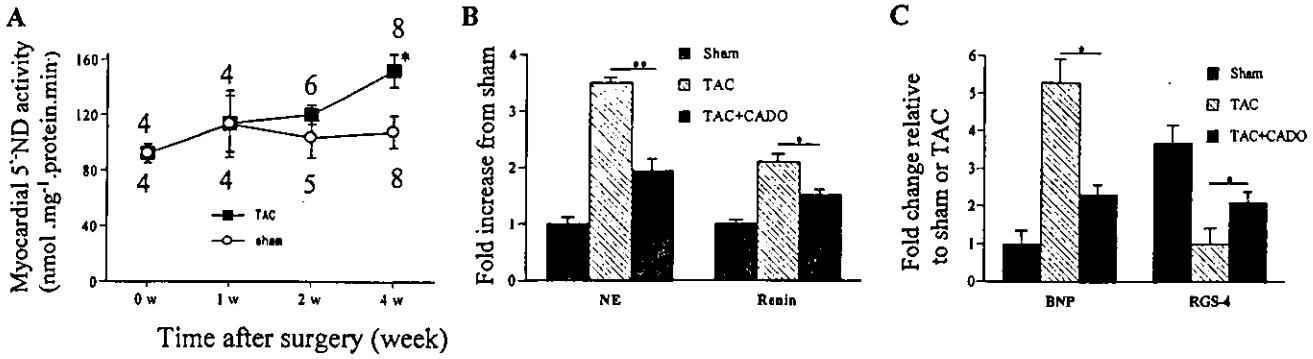

Figure 4. Results of 5'-ND, norepinephrine, renin, and expression of RGS-4 and BNP. A, Time course of myocardial 5'-ND activity. *P<0.05 compared with the sham-operated mice. The number of mice in each time point is indicated above or under the data points. B, Plasma concentrations of NE and renin (n=7 in each group), *P<0.05, **P<0.01 compared with TAC. C, Fold change of gene expression of BNP and RGS-4 (n=4 in each group), *P<0.05 compared with the sham-operated mice. Values are expressed as mean±SEM.

phenomenon. Considering that the EC_{50} of CADO on adenylate cyclase activity mediated by A_1, A_{2A}, and A_{2B} receptors is 100, 460, and 15 000 nmol/L, respectively, and the inhibitory effects of CADO are mimicked by CPA (A_1 receptor selective agonist) and NECA (A_1, A_{2A}, and A_{2B} receptor agonist) but not CGS21680 (A_{2A} receptor selective agonist), the inhibitory effects of adenosine on protein synthesis are most likely mediated via A_1 receptors rather than A_{2A} receptors. However, mediation via the A_{2B} receptor cannot be completely ruled out because the low affinity of CADO for the A_{2B} receptor makes it unlikely that the stimulation of A_{2B} receptors mediates myocardial antihypertrophy produced by CADO. Furthermore, our in vivo studies using a selective adenosine A_1 agonist, CPA, and an antagonist, DPCPX, clearly showed that the stimulation of A_1 receptors mainly mediates the antihypertrophic effect of CADO. Moreover, there is a substantial

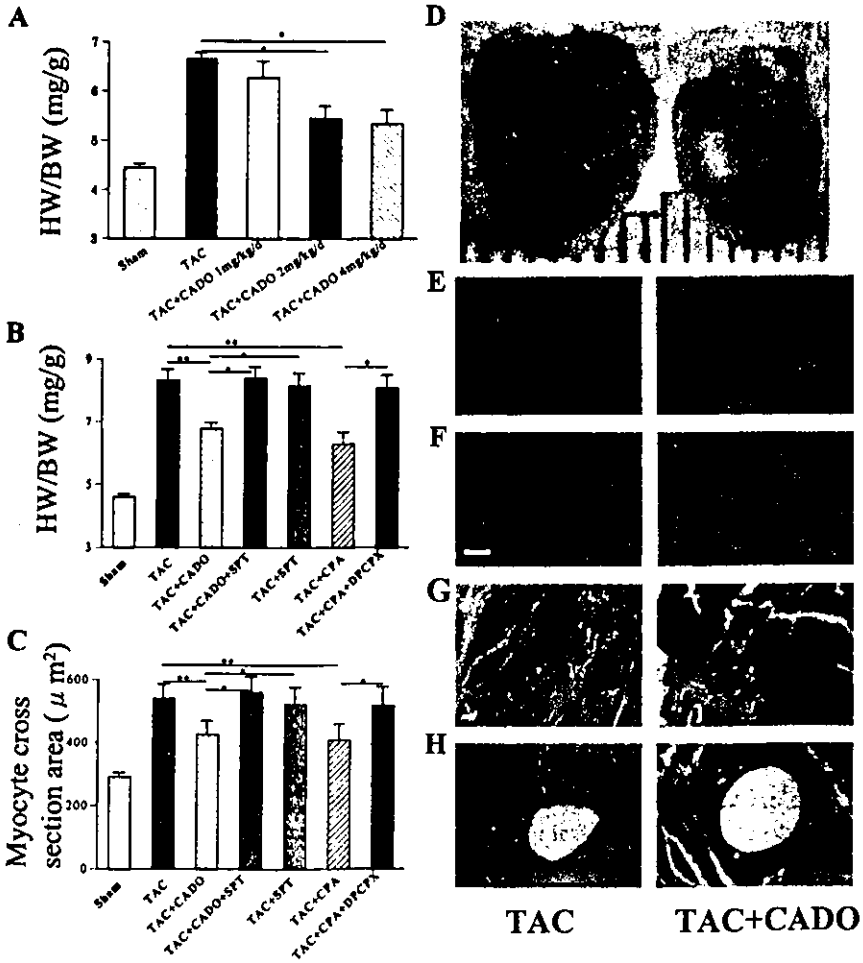

Figure 5. Inhibition of myocardial hypertrophy and fibrosis in vivo by CADO. A, Heart weight to body weight (HW/BW) ratio was attenuated in a dose-dependent fashion by CADO after 1 week of TAC. *P<0.05, n=10 and 7 in sham and TAC groups, respectively; n=5 in the 3 different dose CADO groups. B, HW/BW was attenuated by CADO or CPA treatment after 4 weeks, *P<0.01, **P<0.0001. The number of mice in sham, TAC, TAC+CADO, TAC+CADO+SPT, TAC+SPT, TAC+CPA, and TAC+CPA+DPCPX groups is 28, 29, 20, 8, 12, 5, and 6, respectively. C, Cardiomyocyte cross-sectional area was decreased in CADO- or CPA-treated mice after 4 weeks, *P<0.05, **P<0.01. The number of mice in sham, TAC, TAC+CADO, TAC+CADO+SPT, TAC+SPT, TAC+CPA, and TAC+CPA+DPCPX group is 9, 11, 8, 5, 6, 5, and 6, respectively. D, Representative hearts of mice treated with TAC or TAC+CADO for 4 weeks (scale bar=1 mm). E and F, H&E staining of heart tissues (scale bar=20 μm). Myocardial (G) or perivascular (H) fibrosis (Azan-Mallory stain, bar=20 μm). Values are mean±SEM.

Hemodynamics and Echocardiographic Results at 4 Weeks

	TAC (n=22)	TAC+SPT+CADO (n=7)	TAC+SPT (n=17)	TAC+CADO (n=15)	TAC+CPA (n=6)	TAC+CPA +DPCPX (n=6)	Sham (n=14)
BW, g	23.2±0.47†	21.1±0.31†	22.5±0.46†	22.6±0.34†	22.8±0.44†	22.2±0.6†	24.6±0.24
HR, bpm	645±26.8	614±32.6	678±22.2	643±11.4	680±17	680±18	671±11.4
SBP, mm Hg	104±3.7	104±3.7	102±3.1*	107±1.8	100±8	94±5*	114±3.0
δBP, mm Hg	51±6	49±4	49±5	47±6	48±5	46±7	5±3
PWTd, mm	1.04±0.05†§¶	0.99±0.02†§	1.01±0.06†§	0.85±0.03†	0.75±0.01	0.94±0.04†#	0.66±0.02
LVEDd, mm	3.35±0.13*‡¶	3.34±0.15*‡	3.35±0.16*‡	3.24±0.10	3.21±0.09	3.47±0.13*¶	3.16±0.12
LVESd, mm	2.30±0.14*‡¶	2.32±0.15*‡	2.31±0.18*‡	2.06±0.10	1.98±0.11	2.35±0.15*¶	1.95±0.12
%PWT	24.8±4.2†§¶	23.4±3.3†§	28.8±6.5	41.4±4.5	42.3±5.2	22.7±6.4†¶	42.7±7.6

SPT indicates 8-(*p*-sulfophenyl)-theophylline; HR, heart rate; SBP, systolic blood pressure; δBP, *trans*-stenosis pressure gradient (n=3 to 4 in every group); TAC, transverse aortic constriction; PWTd, left ventricular (LV) diastolic posterior wall thickness; LVEDd, LV end-diastolic dimension; LVESd, LV end-systolic dimension; %PWT, percentage of increase in PWTs relative to PWTd; and FS, left ventricular fractional shortening. *$P<0.05$, †$P<0.01$ vs Sham; ‡$P<0.05$, §$P<0.01$ vs TAC+CADO; ¶$P<0.01$ vs TAC+CPA. Data are mean±SEM.

body of evidence suggesting that the stimulation of A_1 receptors mediates antigrowth effect. Adenosine-induced inhibition of norepinephrine release from adrenergic nerves in the heart is also mediated via the A_1 receptor[27] and has an antiadrenergic effect on hypertrophy caused by pressure overload,[16] consistent with the result in this study that plasma norepinephrine was reduced by CADO treatment. Interestingly, the activation of adenosine A_1 receptors has been reported to be able to inhibit cardiac cell proliferation and lead to cardiac hypoplasia in cultured whole murine embryos.[28] We were also able to demonstrate in this study that CADO can inhibit protein kinase A–dependent hypertrophic signaling. Iso stimulates hypertrophy by activation of adrenergic β receptors, and this stimulation leads to the activation of adenylate cyclase and subsequently induces hypertrophy. The stimulation of adenosine A_1 receptors is known to inhibit adenylate cyclase, which therefore may be an alternative mechanism for CADO-induced attenuation of hypertrophy. To clarify this point, we used forskolin, the most potent AC stimulator, to stimulate protein synthesis of myocytes. As expected, CADO completely eliminated any increase in the protein synthesis induced by forskolin. We therefore posit that the signaling of A_1 receptor activation is linked with both G_o and G_i proteins and that inhibition of adenylate cyclase may suppress the hypertrophic signaling pathways in cardiomyocytes.

It has become clear that the development of cardiac hypertrophy is a multigenic, integrative response involving signal integration of multiple pathways. The antihypertrophic effect of CADO could also be attributable, in part, to a reduction of $[Ca^{2+}]_i$ in myocytes,[16] because $[Ca^{2+}]_i$ can stimulate the calcineurin-mediated cardiac hypertrophic pathway.[9] Even more interesting is that RGS, which attenuates G protein–mediated signaling, may also be an alternative pathway through which CADO can inhibit G_q protein–induced hypertrophy, because it is reported that an increase in cAMP level resulted in a reduction of the RGS-4 message by nearly 50%.[29] We also confirmed in this study that expression of RGS-4 was upregulated by CADO treatment. Thus, CADO may exert an antihypertrophic effect mediated by increasing RGS-4 via the inhibition of adenylate cyclase.

Our results indicate that CADO not only attenuates cardiac hypertrophy but also dramatically improves heart function, which is consistent with our findings in patients with heart failure as previously reported.[19] The antiadrenergic effect of CADO is likely to protect the heart in a way similar to that of the adrenergic β blocker by reducing either contractility or heart rate. Moreover, CADO may be superior to β blocker because it can attenuate the activation of renin-angiotensin system[14] and counteract TNF-α.[15] On the other hand, we also should notice that A_1 adenosine antagonist BG9719 was reported to preserve renal function via promoting natriuresis during treatment for heart failure.[30] Reducing glomerular filtration rate should be considered one of the adverse effects of adenosine A_1 agonists, but it is not enough to deny the potential beneficial affects of adenosine receptor activation on heart failure mediated by their well-known antiadrenergic effect. Nevertheless, a recent study revealed that no significant difference on glomerular filtration rate was noted between A_1 receptor deficiency mice and wild-type mice.[25] In this study, we have noted a positive correlation between cardiac hypertrophy and pulmonary congestion, indicating that the beneficial effect of CADO on preventing heart failure at least partially should be attributed to its inhibitory effect on myocardial hypertrophy. Although this seems paradoxical to the traditional notion that hypertrophy is a needed compensatory mechanism, recent studies on murine TAC model suggest that cardiac hypertrophy is not a required compensatory response to pressure overload.[31,32]

We have characterized the time course of LVH and heart function changes in a previous study[21] and showed that significant LVH and impaired LV heart function (FS) appeared at 4 weeks after TAC. In this study, we noted that myocardial 5′-ND activity was also increased significantly at 4 weeks, a time course in good accordance with FS, suggesting that declined heart function is associated with increased 5′-ND activity. This observation is in agreement with the clinical investigation.[18] Although in this study we did not find that 8-SPT additionally increases cardiac hypertrophy and decelerates the heart function in the TAC model, the cardioprotection of adenosine cannot be excluded because the concentration of endogenous adenosine may be far below the

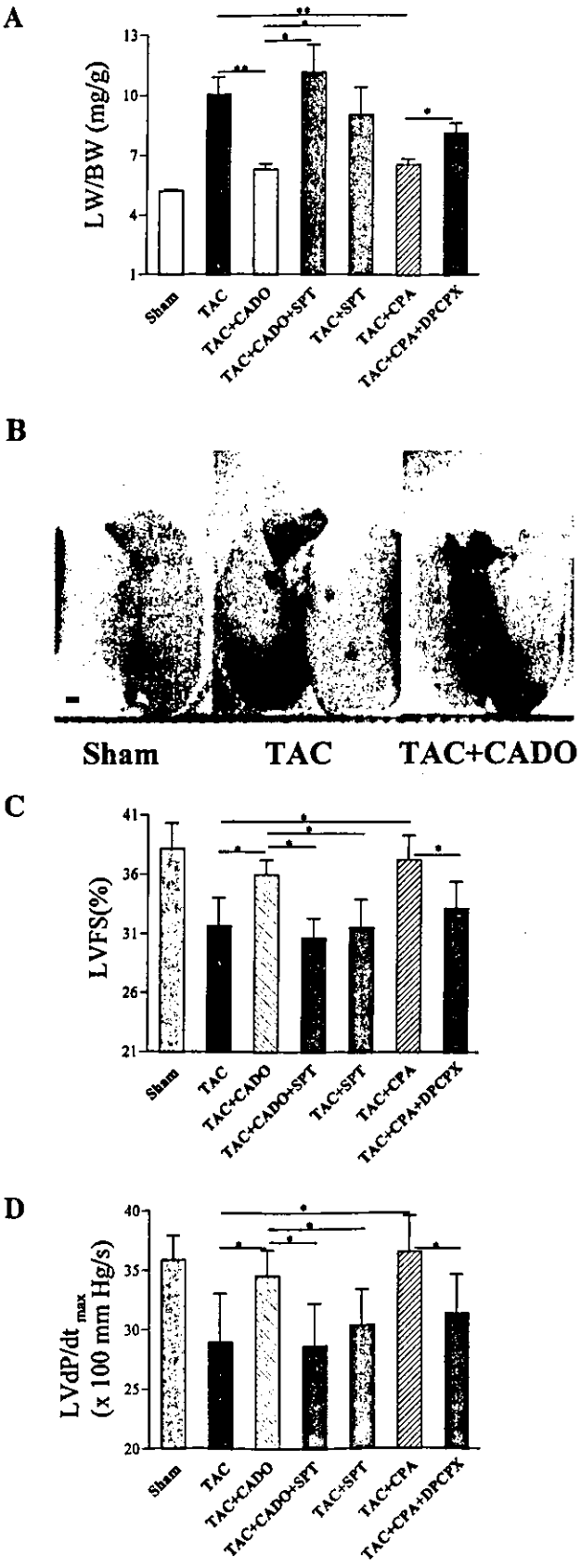

Figure 6. Improvement of heart function in vivo by CADO. A, Lung weight to body weight (LW/BW) ratio was attenuated by CADO or CPA. *$P<0.01$, **$P<0.0001$. Numbers of mice in every group and abbreviations are the same as in Figure 5B. B, Representative lungs of mice treated with sham, TAC, or TAC+CADO (bar=1 mm). C, LVFS. *$P<0.05$. The number of mice in sham, TAC, TAC+CADO, TAC+CADO+SPT, TAC+SPT, TAC+CPA, and TAC+CPA+DPCPX groups is 14, 22, 15, 7, 17, 6, and 6 respectively. D, LV dP/dt_{max} was increased in CADO- or CAP-treated mice. *$P<0.05$, n=5 in every group. Values are mean±SEM.

level to be able to act at the receptor level in pressure-overload state. Therefore, it would be of importance to clarify whether augmentation of endogenous adenosine is beneficial to cardiac hypertrophy.

In conclusion, the data in this study indicate that the activation of adenosine A_1 receptors attenuates both the cardiac hypertrophy and myocardial dysfunction mediated by combined mechanisms of antiadrenergic effect and upregulation of RGS-4.

Acknowledgments

This work was supported by Grants-in-Aid for Scientific Research (Nos. 12470153 and 12877107) from the Japanese Ministry of Education, Culture, Sports, Science and Technology; Human Genome, Tissue Engineering and Food Biotechnology (H13-Genome-011) in Health and Labor Sciences Research Grants, and Comprehensive Research on Aging and Health (H13-21seiki [seikatsu]-23) in Health and Labor Sciences Research Grants from the Ministry of Health and Labor and Welfare, Japan. This work was also supported by Research on Health Technology Assessment (H14-iryo-025) in Health and Labor Sciences Research Grants from the Ministry of Health and Labor and Welfare, Japan. The authors would like to thank Tomi Fukushima and Junko Yamada for expert technical assistance.

References

1. Sadoshima J, Izumo S. Molecular characterization of angiotensin II–induced hypertrophy of cardiac myocytes and hyperplasia of cardiac fibroblasts: critical role of the AT_1 receptor subtype. *Circ Res.* 1993;73:413–423.
2. Akers WS, Cross A, Speth R, Dwoskin LP, Cassis LA. Renin-angiotensin system and sympathetic nervous system in cardiac pressure-overload hypertrophy. *Am J Physiol Heart Circ Physiol.* 2000;279:H2797–H2806.
3. Dostal DE, Baker KM. Angiotensin and endothelin: messengers that couple ventricular stretch to the Na^+/H^+ exchanger and cardiac hypertrophy. *Circ Res.* 1998;83:870–873.
4. Schafer M, Ponicke K, Heinroth-Hoffmann I, Brodde OE, Piper HM, Schluter KD. β-Adrenoceptor stimulation attenuates the hypertrophic effect of α-adrenoceptor stimulation in adult rat ventricular cardiomyocytes. *J Am Coll Cardiol.* 2001;37:300–307.
5. Deng XF, Rokosh DG, Simpson PC. Autonomous and growth factor-induced hypertrophy in cultured neonatal mouse cardiac myocytes: comparison with rat. *Circ Res.* 2000;87:781–788.
6. Asakura M, Kitakaze M, Takashima S, Liao Y, Ishikura F, Yoshinaka T, Ohmoto H, Node K, Yoshino K, Ishiguro H, Asanuma H, Sanada S, Matsumura Y, Takeda H, Beppu S, Tada M, Hori M, Higashiyama S. Cardiac hypertrophy is inhibited by antagonism of ADAM12 processing of HB-EGF: metalloproteinase inhibitors as a new therapy. *Nat Med.* 2002;8:35–40.
7. Patel R, Lim DS, Reddy D, Nagueh SF, Lutucuta S, Sole MJ, Zoghbi WA, Quinones MA, Roberts R, Marian AJ. Variants of trophic factors and expression of cardiac hypertrophy in patients with hypertrophic cardiomyopathy. *J Mol Cell Cardiol.* 2000;32:2369–2377.
8. Meguro T, Hong C, Asai K, Takagi G, McKinsey TA, Olson EN, Vatner SF. Cyclosporine attenuates pressure-overload hypertrophy in mice while enhancing susceptibility to decompensation and heart failure. *Circ Res.* 1999;84:735–740.

9. Yatani A, Honda R, Tymitz KM, Lalli MJ, Molkentin JD. Enhanced Ca^{2+} channel currents in cardiac hypertrophy induced by activation of calcineurin-dependent pathway. *J Mol Cell Cardiol.* 2001;33:249–259.
10. Clerk A, Pham FH, Fuller SJ, Sahai E, Aktories K, Marais R, Marshall C, Sugden PH. Regulation of mitogen-activated protein kinases in cardiac myocytes through the small G protein Rac1. *Mol Cell Biol.* 2001;21: 1173–1184.
11. Nemoto S, Sheng Z, Lin A. Opposing effects of Jun kinase and p38 mitogen-activated protein kinases on cardiomyocyte hypertrophy. *Mol Cell Biol.* 1998;18:3518–3526.
12. Rongen GA, Lenders JW, Lambrou J, Willemsen JJ, Van Belle H, Thien T, Smits P. Presynaptic inhibition of norepinephrine release from sympathetic nerve endings by endogenous adenosine. *Hypertension.* 1996;27: 933–938.
13. Stowe DF, O'Brien WC, Chang D, Knop CS, Kampine JP. Reversal of endothelin-induced vasoconstriction by endothelium-dependent and -independent vasodilators in isolated hearts and vascular rings. *J Cardiovasc Pharmacol.* 1997;29:747–754.
14. Taddei S, Arzilli F, Arrighi P, Salvetti A. Dipyridamole decreases circulating renin-angiotensin system activity in hypertensive patients. *Am J Hypertens.* 1992;5:29–31.
15. Wagner DR, McTiernan C, Sanders VJ, Feldman AM. Adenosine inhibits lipopolysaccharide-induced secretion of tumor necrosis factor-α in the failing human heart. *Circulation.* 1998;97:521–524.
16. Meyer TE, Chung ES, Perlini S, Norton GR, Woodiwiss AJ, Lorbar M, Fenton RA, Dobson JG Jr. Antiadrenergic effects of adenosine in pressure overload hypertrophy. *Hypertension.* 2001;37:862–868.
17. Dubey RK, Gillespie DG, Mi Z, Jackson EK. Exogenous and endogenous adenosine inhibits fetal calf serum-induced growth of rat cardiac fibroblasts: role of A_{2B} receptors. *Circulation.* 1997;96:2656–2666.
18. Funaya H, Kitakaze M, Node K, Minamino T, Komamura K, Hori M. Plasma adenosine levels increase in patients with chronic heart failure. *Circulation.* 1997;95:1363–1365.
19. Kitakaze M, Minamino T, Node K, Koretsune Y, Komamura K, Funaya H, Kuzuya T, Hori M. Elevation of plasma adenosine levels may attenuate the severity of chronic heart failure. *Cardiovasc Drugs Ther.* 1998;12:307–309.
20. Simpson P, McGrath A, Savion S. Myocyte hypertrophy in neonatal rat heart cultures and its regulation by serum and by catecholamines. *Circ Res.* 1982;51:787–801.
21. Liao Y, Ishikura F, Beppu S, Asakura M, Takashima S, Asanuma H, Sanada S, Kim J, Ogita H, Kuzuya T, Node K, Kitakaze M, Hori M. Echocardiographic assessment of LV hypertrophy and function in aortic-banded mice: necropsy validation. *Am J Physiol Heart Circ Physiol.* 2002;282:H1703–H1708.
22. Ding B, Price RL, Borg TK, Weinberg EO, Halloran PF, Lorell BH. Pressure overload induces severe hypertrophy in mice treated with cyclosporine, an inhibitor of calcineurin. *Circ Res.* 1999;84:729–734.
23. Choi DJ, Koch WJ, Hunter JJ, Rockman HA. Mechanism of β-adrenergic receptor desensitization in cardiac hypertrophy is increased β-adrenergic receptor kinase. *J Biol Chem.* 1997;272:17223–17229.
24. Kitakaze M, Node K, Asanuma H, Takashima S, Sakata Y, Asakura M, Sanada S, Shinozaki Y, Mori H, Kuzuya T, Hori M. Protein tyrosine kinase is not involved in the infarct size-limiting effect of ischemic preconditioning in canine hearts. *Circ Res.* 2000;87:303–308.
25. Brown R, Ollerstam A, Johansson B, Skott O, Gebre-Medhin S, Fredholm B, Persson AE. Abolished tubuloglomerular feedback and increased plasma renin in adenosine A_1 receptor-deficient mice. *Am J Physiol Regul Integr Comp Physiol.* 2001;281:R1362–R1367.
26. Brede M, Wiesmann F, Jahns R, Hadamek K, Arnolt C, Neubauer S, Lohse MJ, Hein L. Feedback inhibition of catecholamine release by two different α_2-adrenoceptor subtypes prevents progression of heart failure. *Circulation.* 2002;106:2491–2496.
27. Snyder DL, Wang W, Pelleg A, Friedman E, Horwitz J, Roberts J. Effect of aging on A_1-adenosine receptor-mediated inhibition of norepinephrine release in the rat heart. *J Cardiovasc Pharmacol.* 1998;31:352–358.
28. Zhao Z, Rivkees SA. Inhibition of cell proliferation in the embryonic myocardium by A_1 adenosine receptor activation. *Dev Dyn.* 2001;221: 194–200.
29. Pepperl DJ, Shah-Basu S, VanLeeuwen D, Granneman JG, MacKenzie RG. Regulation of RGS mRNAs by cAMP in PC12 cells. *Biochem Biophys Res Commun.* 1998;243:52–55.
30. Gottlieb SS, Brater DC, Thomas I, Havranek E, Bourge R, Goldman S, Dyer F, Gomez M, Bennett D, Ticho B, Beckman E, Abraham WT. BG9719 (CVT-124), an A_1 adenosine receptor antagonist, protects against the decline in renal function observed with diuretic therapy. *Circulation.* 2002;105:1348–1353.
31. Hill JA, Karimi M, Kutschke W, Davisson RL, Zimmerman K, Wang Z, Kerber RE, Weiss RM. Cardiac hypertrophy is not a required compensatory response to short-term pressure overload. *Circulation.* 2000;101: 2863–2869.
32. Esposito G, Rapacciuolo A, Naga Prasad SV, Takaoka H, Thomas SA, Koch WJ, Rockman HA. Genetic alterations that inhibit in vivo pressure-overload hypertrophy prevent cardiac dysfunction despite increased wall stress. *Circulation.* 2002;105:85–92.

Circ J 2003; **67**: 788–792

Canine DNA Array as a Potential Tool for Combining Physiology and Molecular Biology

—— An Application for the Gene Expression Profile of Regional Ischemic Myocardium ——

Masanori Asakura, MD; Seiji Takashima, MD; Yoshihiro Asano, MD; Tsuyoshi Honma, PhD**; Hiroshi Asanuma, MD; Shoji Sanada, MD; Yasunori Shintani, MD; Yulin Liao, MD; Jiyoong Kim, MD*; Hisakazu Ogita, MD; Koichi Node, MD; Tetsuo Minamino, MD; Ryosuke Yorikane, PhD**; Akiko Agai, BS*; Soichiro Kitamura, MD*; Hitonobu Tomoike, MD*; Masatsugu Hori, MD; Masafumi Kitakaze, MD*

The combining of molecular biology and physiology is essential for the further development of cardiovascular medicine, and DNA microarray is a useful tool for assessing multiple gene expressions. A canine DNA microarray has been designed and tested. Approximately 60 cardiovascular-related genes were cloned from newly developed canine cDNA libraries and spotted on slides. Using the arrays, the gene expression profiles of canine myocardium in were analyzed 2 protocols: (1) ischemic myocardium by 50% reduction of the coronary blood flow, and (2) necrotic myocardium caused by coronary artery ligation. Three hours after 50% flow reduction, cardiovascular-related genes, including ecto-5'-nucleotidase, endothelin-1, PAI-1, and AT receptors, exhibited rapid alteration and there were many more altered genes than with the complete coronary occlusion. Irreversible ischemic damage without necrosis more strongly affected gene expressions in surviving myocardium than in fatally damaged myocardium. The canine DNA microarray is a useful tool for assessing the precise molecular events following changes in the pathophysiological conditions of the heart. (*Circ J* 2003; **67**: 788–792)

Key Words: DNA microarray; Ischemic myocardium; Necrotic myocardium

It is important to know the pathophysiological response of the heart to different types of stress such as ischemia or pressure/volume overload, but it is difficult to investigate and comprehend because many substances are thought to be involved. In particular, in the cardiovascular field it is essential to know the precise molecular mechanisms of either cardiac injury or cardioprotection and because the genetic expression of proteins or enzymes in stressed hearts is believed to be responsible for the modulation of the levels of cardioactive substances, it is important to examine all of the genes expressed during ischemic stress. Recently, considerable amounts of cDNA were identified in the human and the mouse. Stanton et al[2] and Lyn et al[3] revealed an alteration in the pattern of gene expression in response to myocardial infarction using a novel clustering program in a rat model of old myocardial infarction. However, the rat or murine heart is too small to mimic precise pathophysiological conditions such as myocardial hibernation, coronary hypoperfusion or myocardial stunning. Indeed, because the oxygen supply from blood vessels is essential for the survival of tissues, and an insufficiency because of impaired blood vessels eventually causes tissue damage, it is important to examine which genes are expressed during the various events of myocardial ischemia to understand the cellular mechanisms of both ischemic injury and the cardioprotection afforded by ischemic preconditioning. Therefore, the constitution of the cDNA microarray in a large animal such as a dog is desirable and essential for combining the pathophysiological and molecular biological knowledge of the heart.

In this study, we focused on the development of high-fidelity canine specific cDNA array panels from close-bred specific pathogen frec beagle dogs. For the validation of the usefulness of the cDNA microarray for canine hearts, we analyzed the expression profiles of myocardial genes following reversible and irreversible injury.

(Received March 5, 2003; revised manuscript received June 24, 2003; accepted July 2, 2003)

*Department of Internal Medicine and Therapeutics, Osaka University Graduate School of Medicine, Osaka, *Cardiovascular Division of Internal Medicine, National Cardiovascular Center, Suita and **Pharmacology & Molecular Biology Research Laboratories, Sankyo Co Ltd, Tokyo, Japan*

Mailing address: Masafumi Kitakaze, MD, PhD, Cardiovascular Division of Medicine, National Cardiovascular Center, 5-7-1 Fujishirodai, Suita 565-8565, Japan. E-mail: kitakaze@zf6.so-net.ne.jp

Methods

All procedures were performed in compliance with the Guide for the Care and Use of Laboratory Animals (NIH publication No. 85-23, revised 1985) and approved by the Osaka University Ethical Committee for Laboratory Animal Use.

Canine cDNA Library Construction

Total RNA was extracted from fresh-frozen tissues (heart, lung, brain, kidney, liver, spleen, skeletal muscle, and testis) of beagle dogs using TRIzol reagent (Invitrogen). The mRNA was purified using the PolyATract mRNA

Table 1 Canine cDNA Clones

	Gene Name	Hom.	Canine	Human	Rat	Mouse
1	ET-1	75%		J05008	M64711	D43775
2	ANP		M12045	M54947	M27498	K02781
3	BNP		M31777	M31776	M25297	D16497
4	PAI-1	83%		M16006	M24067	M33960
5	tPA	85%		M15518	M23697	J03520
6	ecto 5'-nucleotidase	91%		NM_002526	J05214	L12059
7	cytosolic 5'-nucleotidase	95%		D38524		
8	adenosine deaminase	90%		K02567	U18942	M10319
9	adenosine kinase	93%		U33936	U57042	U26589
10	Mn SOD	89%		M36693		L35525
11	Cu/Zn SOD	85%		X02317	M25157	M35725
12	nNOS	92%		D16408	U67309	D14552
13	iNOS		AF077821	AF051164	U03699	U43428
14	ecNOS	90%		L26914	D14051	U53142
15	AT1 receptor		P43240	M87290	M87003	
16	AT2 receptor	>99%		U20860	U22663	
17	A1 receptor		X14051	S56143	AF042079	
18	A2α receptor		X14052	U40771	AF228684	
19	A2β receptor	90%		M97759	M91466	NM_007413
20	A3 receptor		U54792			AF069778
21	KDR/Flk-1	89%		AF063658		X70842
22	Flt	91%		E13256	D28498	L07297
23	neuropilin-1	93%		AF018956	AF016296	D50086
24	neuropilin-2	91%		AF022860	AF016297	AF022854
25	EGF receptor	84%		NM_005228	M37394	U03425
26	VEGF		AF133248	AF214570	AF222779	U73620
27	HGF	78%		M73240	NM_017017	D10213
28	HB-EGF	88%		L05489	M60278	NM_010415
29	ICAM-1		L31625	J03132	D00913	M31585
30	P-selectin	77%		NM_003005	L23088	M87861
31	VCAM-1		U32086	M60335	M84488	M84487
32	PKC beta(β)	94%		NM_002738	M19007	
33	PKC gamma(γ)	84%		AF345987	NM_012628	L28035
34	PKC mu(μ)	95%		X75756	AB020616	
35	PKC theta(θ)	90%		NM_006257	(AB020614)	D11091
36	PKC eta(η)	92%		NM_006255		D90242
37	PKC zeta(ζ)	84%		NM_002744	J04532	
38	JNK1	89%		U34822		AB005663
39	JNK2	84%		U34821		AB005664
40	JNK3	90%		U35004		AB005665
41	ERK1	93%		X60188	M61177	X64605
42	ERK2	92%		M84489	M64300	D10939
43	ERK3	95%		X80692	M64301	X64607
44	β2 receptor		U73206	AF203386	L39264	AY011270
45	collagen type1 α1		AF153062	NM_000088	(J04464)	(X54876)
46	collagen type1 α2		AF035120	XM_004658	AF121217	
47	IL-6		U12234	M54894	M26744	J03783
48	TGFβ1		L34956	XM_008912	NM_021578	NM_011577
49	p53		AB020761	AF307851	AY009504	AF161020
50	cardiovascular HSP	84%		AF155908	AF155910	AF155909
51	HSP70	94%		AF093759	L16764	M35021
52	caspase-3	88%		U13737	NM_012922	U19522
53	calcineurin A1	98%		M29550	D90035	
54	calcineurin B	95%		M30773	D14568	
55	calcineurin catalytic subunit	95%		J05480		J05479
56	catarase		AB012918	X04076	M11670	M62897
57	Gαq		L76257	AF329284		M55412
58	β-actin		AF021873	M10277	V01217	M12481
59	GAPDH	90%		XM_006959	AF106860	M32599
60	α-tubulin	95%		AF081484	NM_022298	M13445
61	HPRT	96%		M31642	X62085	J00423
62	phospholipase A2		M35301	AF112982	U38376	AF112984
63	ubiquitin		AB032025	M26880		

Hom, the percentage of homology with the human DNA sequence. "Canine", "Human", "Rat", and "Mouse", the Genebank accession numbers.

isolation System (Promega). Briefly cDNA was synthesized with MMLV-Reverse transferase and fractionated by gel filtration. We constructed 8 canine tissue cDNA libraries.

Cloning of Canine Cardiovascular Related Genes

We selected 57 genes that have been reported as involved in cardiovascular pathophysiology and 6 ubiquitous genes as internal controls (Table 1). For the construction of the canine expression profiles of the cardiovascular-related genes, we cloned the fragments of canine cDNAs for spotting on slides as probes for expression analysis. These probes were all amplified by polymerase chain reaction (PCR) from the canine cDNA library from which was made the 8 mixed tissues. To obtain specific high-output

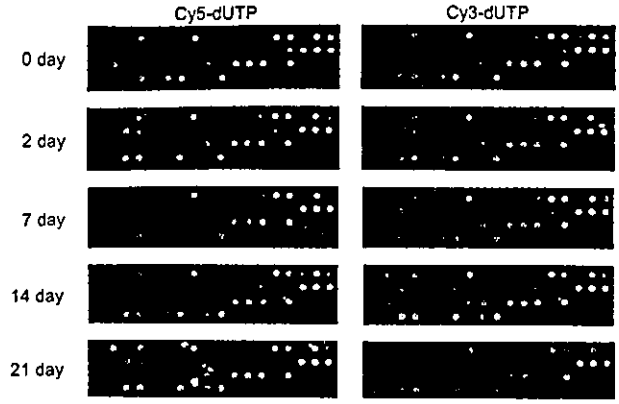

Fig 1. The arrays, which were used 0, 2, 7, 14 and 21 days after they are made, were hybridized with the same samples with 2 different types of labeling as cyanine-3(Cy-3) or cyanine-5(Cy-5) florochrome.

hybridized signals, PCR primers were chosen to amplify the 3' side 500–1,000 bp fragments of the protein-coding regions so as to avoid high homology sequences with other proteins. Although most of the canine cDNA sequences for designing these PCR primers were available from public databases, several unknown canine cDNA fragments were amplified by designated primers from mouse and human sequences and all the amplified fragments were subcloned into pCR2.1 (Invitrogen) vectors and were confirmed as canine sequences.

Canine DNA Microarray

Each probe was re-amplified from these subcloned vectors using the same primers and was spotted from 96-well microtiter plates to CMT-GAPS amino-silane-coated slides (CORNING) using a GMS-417 arrayer (Genetic MicroSystems). After the printed arrays were incubated for 1 h at 37°C in a humidity chamber, they were crosslinked by UV 200 mJ/cm^2. The slides were rinsed once in 0.2% sadium dodecy sulfate (SDS), twice in H_2O, and once in blocking buffer for 20 min. The arrays were rinsed in H_2O, submerged in H_2O at 95°C, transferred into 95% ethanol, and stored in the dark until subsequent hybridization.

Preparation of Myocardial Tissues

Protocol 1 Five beagle dogs (Oriental Yeast, Tokyo, Japan) weighing 9–14 kg were prepared as described previously[4] In the sham operation (control) group, we opened the chests of 2 dogs, performed bypass surgery, and removed the hearts 180 min after surgery. In the coronary hypoperfusion group (n=3), the coronary perfusion pressure (CPP) was reduced so that the coronary blood flow (CBF) was decreased to half that of the controls. The ischemic regions of the hearts were extracted 180 min after surgery and submerged in liquid nitrogen.

Protocol 2 Four beagle dogs were prepared as described in Protocol 1. In 2 dogs, ligation of the left anterior descending coronary artery was performed for 360 min, after which the hearts were reperfused for 30 min, removed and the center of the severely ischemic regions was pooled in liquid nitrogen.

Labeled cDNA Samples

Total RNA was prepared from each heart using TRIzol. Fluorescent-labeled cDNA samples were generated by reverse transcription of total RNA (50 g) in the presence of

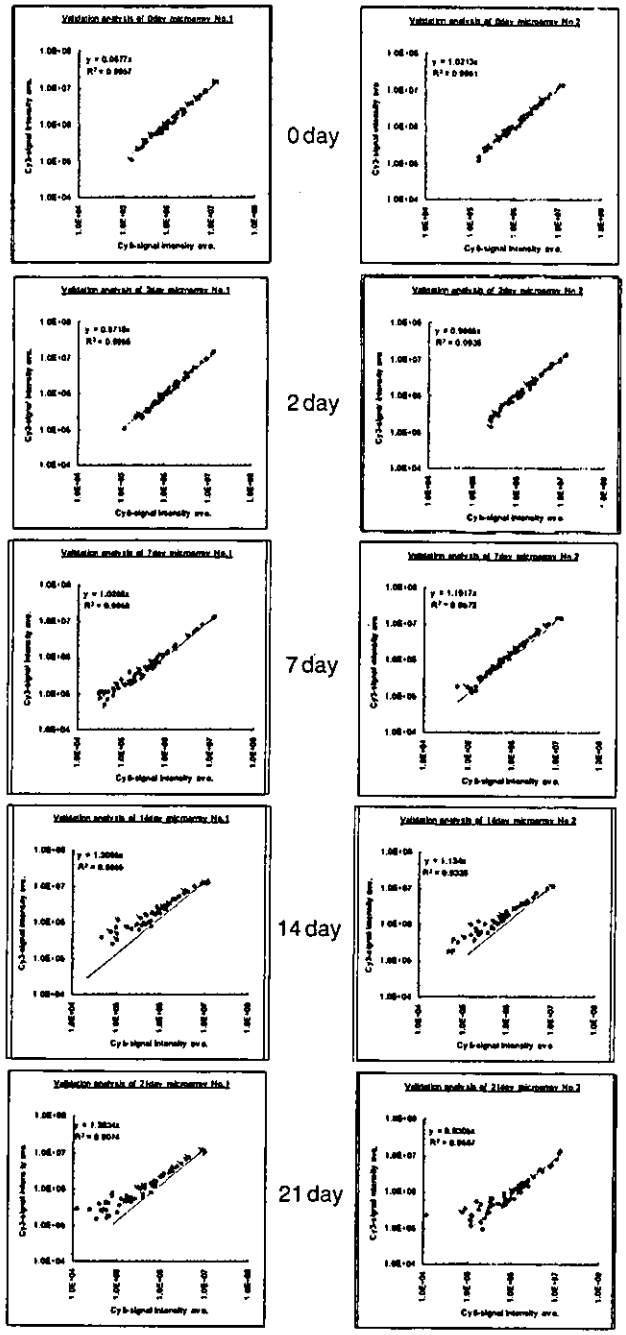

Fig 2. Validation of the canine DNA microarray. Log–log scatterplot of fluorescence measured for mRNA labeled with either cyanine-3 (Cy-3) or cyanine-5 (Cy-5) florochrome in a competitive hybridization on the canine microarrays 0, 2, 7, 14 and 21 days after the microarrays were made.

cyanine-3 (Cy-3) or cyanine-5 (Cy-5)-dUTP using Super Script™ II (Invitrogen).

Array Hybridization and Analysis

The arrays were prehybridized with prehybridization buffer (6×standard saline citrate (SSC), 0.2% SDS, 5× Denhardt's solution, 0.1 mg/ml salmon sperm DNA) for 2 h at room temperature. After washing with 2×SSC, each pair of fluorescent-labeled cDNA sample probes was hybridized to the arrays for 15 h at 65°C. After the arrays were washed with washing buffer (2×SSC, 0.2% SDS) at 55°C,

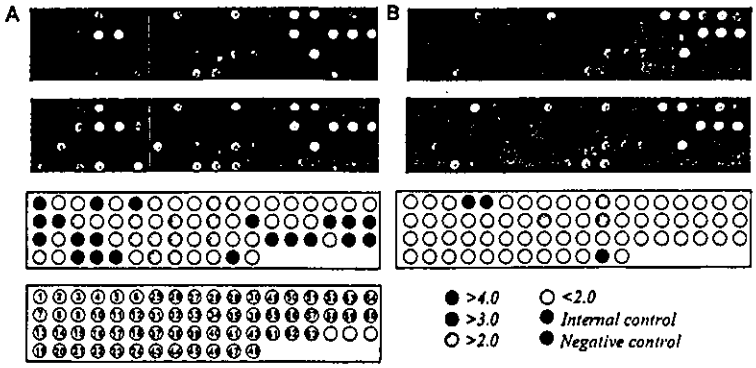

Fig 3. (A) The arrays were hybridized with samples of the control/non-ischemic and low-flow myocardium. The spot numbers are the same numbers on the gene list in Table 1. (B) The arrays hybridized with samples of the control and no-flow myocardium.

the degree of hybridization was quantified by sequential excitation of the 2 fluorophores with a GMS-418 array scanner (Genetic MicroSystems). The results of the scanner were analyzed using Imagene™ (BioDiscovery, ver.3.0). Differential expression values are represented as the ratio of intensities. To assess the stability of the cDNAs on the slide, hybridization was performed immediately and at 7, 14 and 21 days after the slides were freshly blotted.

Results

We constructed the cDNA libraries from various canine tissues to clone canine genes spotted for the cDNA microarrays. All cDNA clones were obtained from canine cDNA libraries (Table 1). The average size of the cDNA clones was 582(212–1,169)bp. The amplified cDNA was sequenced and was confirmed as canine DNA. These canine genes have 78–99% homology to human genes.

To assess the signal reproducibility of the array, we analyzed the hybridization of the same RNA extracted from control canine hearts with differently labeled probes using Cy-3 and Cy-5 (Fig 1). Fig 2 shows the blotted signal intensities of Cy-3 (X-axis) and Cy-5 (Y-axis) for the same blot. There was a close linear relationship of the signal intensities between the Cy-3 and Cy-5 labeled probes immediately or at 7 days after the construction of the arrays. However, the signal linearity was gradually lost using the 14-day-old and 21-day-old arrays. Taking this into consideration, we used only the freshly blotted arrays for the following experiments.

Arrays were probed in duplicate with fluorescent-labeled probes generated from the total RNA extracted from the canine myocardial tissues of the low flow or control groups (Fig 3). The CPP decreased from 103+2 to 52+2 mmHg to obtain the 50% CBF reduction (CBF: 91+2 to 46+1 ml·100^{-1}·min^{-1}). In the control group, CPP (102+1 mmHg) and CBF (92+2 ml·100^{-1}·min^{-1}) did not change. Duplicate results were averaged, discordant or absent results were discarded entirely, and the remaining clones that had increased or decreased by 2-fold relative to control were considered differentially expressed. Six genes (ie, ecto-5'-nucleotidase, endothelin-1, plasminogen activator inhibitor-1 (PAI-1), AT_1 receptor, AT_2 receptor, protein kinase Cq) were up-regulated more than 4-fold compared with the control (Table 2). Seven genes were up-regulated more than 3-fold compared with the controls, and 14 genes were upregulated more than 2-fold, as shown in Table 2.

In contrast to the low-flow model, severe ischemia because of 100% reduction of CBF altered the expression of fewer genes (Table 2). In the more severe ischemia, several genes for cardioprotective substances (ie, ecto-5'-nucleotidase, AT_2 receptor and A_{2a} receptor) were down-regulated, and several genes for cardio-deleterious substances (ie, ET1, adenosine deaminase and PKCgamma) were up-regulated, although both endothelin-1 and PAI-1, which are thought to cause cardiac injury, were down-regulated. These unbalances between the levels of expression of the genes for cardioprotective and cardio-deleterious substances may contribute to the increased severity of myocardial injury when ischemia is prolonged.

Discussion

We first developed a high-fidelity canine cDNA microarray and used it to analyze the expression of 63 genes in reversible ischemic canine hearts. We also confirmed that physiological stimuli such as anesthesia or reversible ischemic injury modulate the expression of cardiovascular-related genes, which suggests that the canine cDNA microarray can be used to identify molecular pathophysiological conditions of the heart. Although decreased CBF relative to myocardial oxygen demand is observed in patients with angina pectoris, this condition cannot be mimicked in mice or rats because the coronary artery of those animals is too small. When precise and accurate hemodynamic changes are required to mimic pathophysiological conditions in the clinical setting, canine hearts can be used to achieve accurate physiological and molecular biological data.

Because myocardial ischemia in rats or mice is induced by 100% ligation of the coronary artery,[5,6] that model is different from the pathological state in human patients with angina pectoris. The gene expressions in ischemia induced by a 50% reduction of CBF, which is similar to human angina pectoris, have not been reported before. We have previously examined the gene expressions of the murine regional ischemic myocardium resulting from coronary ligation,[5,6] but the genes expressed in the non-ischemic myocardium in the mice coronary ligation model are markedly different from those expressed in the substantial canine ischemic myocardium as revealed in the present study. Therefore, we are the first to show the gene expressions in ischemia induced by a 50% reduction in CBF and because the gene expressions are completely different when there is 100% or 50% ligation of the coronary arteries, there appears to be merit in using the canine DNA microarray for investigation of the physiological cause–effect relationship.

Reproducibility is important for the stable analysis of data and we confirmed excellent reproducibility at least for 7 days after the construction of the arrays; however, there

Table 2 Gene Expression in Ischemia

	Gene name	Pair 1	Pair 2	Pair 3
1	ET-1	0.73±0.17	9.2±6.6	1.47±0.24
2	ANP	0.92±0.10	1.2±0.4	1.24±0.14
3	BNP	0.89±0.00	2.3±0.0	0.92±0.12
4	PAI-1	1.05±0.03	4.0±0.7	3.20±0.19
5	tPA	1.08±0.08	1.7±0.2	3.01±0.60
6	ecto 5'-nucleotidase	1.43±0.17	12.2±8.2	1.54±0.18
7	cytosolic 5'-nucleotidase	1.01±0.01	3.0±0.4	1.14±0.20
8	adenosine deaminase	1.30±0.07	3.0±0.2	(1.07)
9	adenosine kinase	0.93±0.03	2.2±0.3	0.80±0.14
10	Mn SOD	0.91±0.07	1.9±0.3	1.01±0.03
11	Cu/Zn SOD	0.88±0.06	1.7±0.3	0.80±0.04
12	nNOS	1.13±0.10	2.0±0.4	1.76±0.03
13	iNOS	1.19±0.10	3.1±0.8	1.54±0.24
14	ecNOS	1.10±0.08	2.2±0.4	1.83±0.07
15	AT1 receptor	1.06±0.58	5.3±1.8	1.21±0.13
16	AT2 receptor	0.68±0.36	6.2±0.5	0.88±0.16
17	A1 receptor	0.99±0.04	1.9±0.3	0.95±0.26
18	A2α receptor	0.98±0.02	2.0±0.2	1.06±0.01
19	A2β receptor	1.29±0.25	2.8±0.3	1.18±0.09
20	A3 receptor	2.50±0.72	(-4.0)	1.79±0.42
21	KDR/Flk-1	1.18±0.03	2.9±0.4	1.41±0.17
22	Flt	1.10±0.01	2.6±0.5	1.22±0.01
23	neuropilin-1	0.93±0.01	2.7±0.1	1.12±0.09
24	neuropilin-2	1.14±0.08	1.9±0.2	1.11±0.22
25	EGF receptor	1.03±0.08	2.4±0.1	1.38±0.18
26	VEGF	1.01±0.03	1.4±0.3	0.75±0.01
27	HGF	1.01±0.11	-4.6±4.5	1.40±0.02
28	HB-EGF	1.06±0.08	2.2±1.2	0.50±0.01
29	ICAM-1	1.26±0.07	2.2±0.5	2.89±0.08
30	P-selectin	0.88±0.20	1.9±0.6	1.70±0.02
31	VCAM-1	1.16±0.09	1.8±0.1	0.95±0.01
32	PKC beta(β)	0.95±0.02	2.4±0.7	2.09±0.44
33	PKC gamma(γ)	1.23±0.20	1.5±0.3	1.39±0.05
34	PKC mu(μ)	1.17±0.04	2.5±1.3	1.22±0.08
35	PKC theta(θ)	1.28±0.17	(5.4)	2.02±0.78
36	PKC eta(η)	1.14±0.03	1.6±0.2	1.19±0.01
37	PKC zeta(ζ)	1.05±0.02	2.5±0.4	1.67±0.14
38	JNK1	1.08±0.02	2.2±0.8	0.80±0.02
39	JNK2	1.20±0.03	1.6±0.6	0.70±0.01
40	JNK3	1.22±0.16	2.8±1.6	0.78±0.13
41	ERK1	1.11±0.04	1.4±0.2	0.87±0.03
42	ERK2	1.12±0.05	1.4±0.4	0.87±0.02
43	ERK3	1.19±0.00	2.4±0.6	0.97±0.17
44	β2 receptor	1.24±0.19	2.7±1.6	1.14±0.08
45	collagen type1 α1	1.09±0.01	1.5±0.2	1.30±0.15
46	collagen type1 α2	1.09±0.00	1.2±0.2	1.14±0.03
47	IL-6	1.15±0.05	3.5±0.6	9.41±1.14
48	TGFβ1	1.12±0.12	1.1±0.2	1.48±0.06
49	p53	1.17±0.00	1.4±0.1	1.48±0.06
50	cardiovascular HSP	1.04±0.03	1.0±0.1	0.58±0.00
51	HSP70	1.09±0.01	1.0±0.2	0.60±0.01
52	caspase-3	1.23±0.00	1.0±0.1	0.52±0.01
53	calcineurin A1	1.18±0.01	0.9±0.2	0.80±0.04
54	calcineurin B	1.21±0.06	1.5±0.3	1.03±0.00
55	calcineurin catalytic subunit	1.21±0.05	1.5±0.3	1.15±0.00
56	catarase	1.06±0.07	0.9±0.2	0.65±0.01
57	Gaq	1.27±0.04	1.3±0.3	1.04±0.03
58	β-actin	0.77±0.02	0.9±0.1	0.80±0.00
59	GAPDH	0.75±0.00	1.2±0.0	0.76±0.05
60	α-tubulin	0.93±0.02	0.9±0.1	0.97±0.05
61	HPRT	1.13±0.00	1.2±0.3	0.89±0.00
62	phospholipase A2	1.12±0.05	1.2±0.2	0.94±0.05
63	ubiquitin	1.03±0.00	0.8±0.1	0.78±0.06

Pair 1, the ratio of hybridization signal intensity of two identical samples from the canine heart; Pair 2, the ratio of gene expressions of low-flow myocardium to normal flow myocardium; Pair 3, the ratio of gene expressions (360 min ligation/360 min sham). All pairs were analyzed twice with three different arrays.

was loss of reproducibility by 14 days and because this relative short life span is thought to be related to the character of the CMT-GAPS coated microglass plates, we may consider changing the microglass plates to prolong the life of the arrays.

The expression of approximately 50% of the genes was altered under ischemic conditions and some of the upregulated genes have been reported in our previous work. Indeed, we have already reported that ecto-5'-nucleotidase, which is the most up-regulated gene in this array, is up-regulated in dogs. Interestingly, the up-regulation of endothelin-1 detected in the present study corresponds with the results of a previous report in human ventricular myocytes of patients with ischemic cardiomyopathy, but not idiopathic dilated caridomyopathy? The down-regulation of hepatocyte growth factor (HGF) in this array does not concur with previous data that myocardial ischemia and reperfusion induce HGF expression in the rat heart[8] but as the present system enables assessment of the relative extent of the increase in the expression of the genes, it may be able to estimate the relative importance of HGF in ischemic hearts. Furthermore, this system can be applied to other pathophysiological conditions, such as cardiac hypertrophy or cardiac failure, as well as for evaluating the effects of certain drugs on the gene expression of the heart.

Study Limitation

We spotted 57 ischemia-related genes and 6 control genes to the arrays, but as it is speculated that approximately 30,000 genes exist in the human genome, we need to develop up to 30,000 canine genes in the arrays. Nevertheless, the importance of the present study is in proposing the necessity of establishing the canine cDNA array system to better understand cardiovascular (patho) physiology from the viewpoint of molecular biology.

Acknowledgments

This study was supported by either Grants on Human Genome, Tissue Engineering and Food Biotechnology (H13-Genome-011) or Grants on Comprehensive Research on Aging and Health (H13-21seiki (seikatsu)-23), in Health and Labour Sciences Research from Ministry of Health, Labour and Welfare, Grant-in-Aid for Scientific Research (12470153 and 12877107) from the Ministry of Education, Culture, Sports, Science and Technology, Japan. M Asakura is a recipient of the Japan Society for the Promotion of Science Research Fellowship.

References

1. Johnatty SE, Dyck JR, Michael LH, Olson EN, Abdellatif M. Identification of genes regulated during mechanical load-induced cardiac hypertrophy. *J Mol Cell Cardiol* 2000; **32:** 805–815.
2. Stanton LW, Garrard LJ, Damm D, Garrick BL, Lam A, Kapoun AM, et al. Altered patterns of gene expression in response to myocardial infarction. *Circ Res* 2000; **86:** 939–945.
3. Lyn D, Liu X, Bennett NA, Emmett NL. Gene expression profile in mouse myocardium after ischemia. *Physiol Genomics* 2000; **2:** 93–100.
4. Kitakaze M, Minamino T, Node K, Komamura K, Shinozaki Y, Mori H, et al. Beneficial effects of inhibition of angiotensin-converting enzyme on ischemic myocardium during coronary hypoperfusion in dogs. *Circulation* 1995; **92:** 950–961.
5. Kitakaze M, Asakura M, Sakata Y, Asanuma H, Sanada S, Kuzuya T, et al. cDNA array hybridization reveals cardiac gene expression in acute ischemic murine hearts. *Cardiovasc Drugs Ther* 2001; **15:** 125–130.
6. Asakura M, Kitakaze M, Sakata Y. Adenosine-induced cardiac gene expression of ischemic murine hearts revealed by cDNA array hybridization. *Circ J* 2002; **66:** 93–96.
7. Serneri GG, Cecioni I, Vanni S, Paniccia R, Bandinelli B, Vetere A, et al. Selective upregulation of cardiac endothelin system in patients with ischemic but not idiopathic dilated cardiomyopathy: Endothlin-1 system in the human failing heart. *Circ Res* 2000; **86:** 377–385.
8. Ono K, Matsumori A, Shioi T, Furukawa Y, Sasayama S. Enhanced expression of hepatocyte growth factor/c-Met by myocardial ischemia and reperfusion in a rat model. *Circulation* 1997; **95:** 2552–2558.

ADAMTS-13 cysteine-rich/spacer domains are functionally essential for von Willebrand factor cleavage

Kenji Soejima, Masanori Matsumoto, Koichi Kokame, Hideo Yagi, Hiromichi Ishizashi, Hiroaki Maeda, Chikateru Nozaki, Toshiyuki Miyata, Yoshihiro Fujimura, and Tomohiro Nakagaki

A severe lack of von Willebrand factor–cleaving protease (VWF-CP) activity can cause thrombotic thrombocytopenic purpura (TTP). This protease was recently identified as a member of the ADAMTS family, ADAMTS-13. It consists of a pre-proregion, a metalloprotease domain, a disintegrin-like domain, a thrombospondin type-1 motif (Tsp1), a cysteine-rich domain, a spacer domain, additional Tsp1 repeats, and CUB domains. To explore the structural and functional relationships of ADAMTS-13, we prepared here 13 sequential COOH-terminal truncated mutants and a single-point mutant (ArgGlyAsp [RGD] to ArgGlyGlu [RGE] in the cysteine-rich domain) and compared the activity of each mutant with that of the wild-type protein. The results revealed that the truncation of the cysteine-rich/spacer domains caused a remarkable reduction in VWF-CP activity. We also prepared immunoglobulin G (IgG) fractions containing inhibitory autoantibodies against ADAMTS-13 from plasma from 3 patients with acquired TTP, and we performed mapping of their epitopes using the aforementioned mutants. The major epitopes of these antibodies were found to reside within the cysteine-rich/spacer domains. These results suggest that the ADAMTS-13 cysteine-rich/spacer domains are essential for VWF-CP activity. (Blood. 2003;102: 3232-3237)

Introduction

Von Willebrand factor (VWF) functions as a molecular glue through its anchoring of platelets at sites of injured vessel walls under high shear stress.[1] Mature VWF contains 2050–amino acid residues, has a molecular weight of approximately 250 kDa, and is released from endothelial cells as an "unusually large" multimer (UL-VWFM) with a molecular weight of approximately 30 000 kDa.[2-5] In healthy individuals, UL-VWFM is converted rapidly in the circulation to smaller forms, a series of multimers with molecular weights ranging from approximately 500 to 20 000 kDa.[6] It is known that the larger multimers have more potent biologic activity.[7,8] Under shear stress conditions in the circulation, VWF becomes more susceptible to proteolysis,[9-12] resulting in the formation of small but consistent proportions of 176-kDa and 140-kDa fragments derived from the approximately 250-kDa VWF subunit.[13] On the basis of these findings, the existence of a specific VWF-cleaving protease (VWF-CP) has been proposed.

UL-VWFM has been found in plasma from patients with thrombotic thrombocytopenic purpura (TTP).[14] TTP is characterized by thrombocytopenia, microangiopathic hemolytic anemia, renal failure, neurologic dysfunction, and fever.[15] In 1996, a metalloprotease that cleaves a peptide bond between amino acid residues Tyr842 and Met843 within the VWF A2 domain was partially purified.[16,17] It was also reported that a deficiency in VWF-CP activity was associated with TTP.[18] On the basis of these findings, it was proposed that the UL-VWFM produced as a result of the deficiency in VWF-CP activity promotes microvascular thrombus formation. Congenital or acquired deficiency of VWF-CP activity can cause TTP. Congenital TTP with neonatal onset and frequent relapses is often diagnosed as Upshaw-Schulman syndrome,[19] and symptoms of acquired TTP develop idiopathically in association with infection, pregnancy, or autoimmune disease. In addition, most adults with TTP have autoantibodies that inhibit VWF-CP activity.[20-22]

In 2001, VWF-CP was purified and its partial NH_2-terminal amino acid sequence was determined.[23-25] On the basis of this sequence, the full-length cDNA for VWF-CP was cloned.[25,26] These findings revealed that VWF-CP is a new member, designated ADAMTS-13, of the ADAMTS family of metalloproteases,[24-26] named for a disintegrin-like and metalloprotease with thrombospondin type I motif. Positional cloning of a gene responsible for congenital TTP also identified the *ADAMTS13* gene.[27]

The human *ADAMTS13* gene spans approximately 37 kb on chromosome 9q34 and contains 29 exons. mRNA encoding ADAMTS-13 spans approximately 5 kb. Studies by Northern blot,[25-28] polymerase chain reaction (PCR) amplification,[26-29] and living-donor–related liver transplantation[30] indicated that ADAMTS-13 is produced primarily in the liver and then released into the circulation. Also, it is known that ADAMTS-13

From the First Research Department, The Chemo-Sero-Therapeutic Research Institute, Kumamoto, Japan; Department of Blood Transfusion Medicine, Nara Medical University, Nara, Japan; National Cardiovascular Center Research Institute, Osaka, Japan; and Department of Health Science, Nara Medical University, Nara, Japan.

Submitted March 27, 2003; accepted July 8, 2003. Prepublished online as *Blood* First Edition Paper, July 17, 2003; DOI 10.1182/blood-2003-03-0908.

Supported in part by research grants from the Ministry of Education, Culture, Sports, Science and Technology of Japan (M.M., K.K., T.M.) and the Ministry of Health, Labor and Welfare of Japan for Blood Coagulation Abnormalities (H14-02) (T.M., Y.F.).

K.S. and M.M. contributed equally to this study.

Reprints: Kenji Soejima, First Research Department, The Chemo-Sero-Therapeutic Research Institute, Kawabe, Kyokushi, Kikuchi, Kumamoto 869-1298, Japan; e-mail: soejima@kaketsuken.or.jp.

The publication costs of this article were defrayed in part by page charge payment. Therefore, and solely to indicate this fact, this article is hereby marked "advertisement" in accordance with 18 U.S.C. section 1734.

rapidly cleaves UL-VWFM on the endothelial cell surface under flowing conditions.[31]

ADAMTS-13 comprises 1427 amino acid residues and consists of a preproregion, a reprolysin-like metalloprotease domain, a disintegrin-like domain, a thrombospondin type-1 motif (Tsp1), a cysteine-rich domain, a spacer domain, 7 additional Tsp1 repeats, and 2 CUB domains.[25-28] The cysteine-rich domain contains the ArgGlyAsp (RGD) sequence, which is widely used for the recognition of integrin.[32]

Recently, we reported 5 mutations in the *ADAMTS13* gene found in 2 families with Upshaw-Schulman syndrome. The effects of these mutations were confirmed by recombinant expression analysis of these ADAMTS-13 mutants. Two mutants, Arg268Pro and Cys508Tyr, when expressed in cultured HeLa cells, had diminished activity caused by secretion disturbances, and 2 other mutants, Gln449Xaa and Pro475Ser, had very low VWF-CP activity despite normal secretion, whereas Gln448Glu showed no difference from the wild-type ADAMTS-13 in VWF-CP activity.[33]

Several alternatively spliced and/or COOH-terminal truncated ADAMTS-13 isoforms may exist in vivo.[23,25-27] Although a considerable amount of data have been accumulated on the properties of ADAMTS-13, little is known about the structural and functional relationship of ADAMTS-13.

In this study, we prepared 13 sequential COOH-terminal truncated molecules and a single point mutant (ArgGlyAsp [RGD] to ArgGlyGlu [RGE] in the cysteine-rich domain) and compared the activity of each mutant protein with that of wild-type recombinant ADAMTS-13. Furthermore, we prepared immunoglobulin G (IgG) fractions containing inhibitory autoantibodies against ADAMTS-13 from the plasma of 3 patients with acquired TTP and performed epitope mapping using the above mutants. These results suggest that the ADAMTS-13 cysteine-rich/spacer domains are essential for expression of VWF-CP activity.

Materials and methods

Construction of expression plasmids of ADAMTS-13 mutants

PCR-based mutagenesis was performed for the construction of ADAMTS-13 mutants as previously described.[33] The mutant cDNA was cloned into the mammalian expression vector pCAGG-neo.[34,35] The DNA sequence of all inserts was confirmed by DNA sequencing.

Transient expression of ADAMTS-13 mutants

Each of the mutant expression plasmids was transfected into HeLa cells by using the polyamine transfection reagent TransIT-LT1 (Mirus, Madison, WI) according to the manufacturer's instructions. Briefly, HeLa cells were cultured in Dulbecco modified Eagle medium (DMEM; Sigma, St Louis, MO) supplemented with 10% fetal bovine serum. Two micrograms of each expression plasmid was transfected into 40% to 70% confluent cells in a 35-mm well. After a 6-hour incubation, the medium was replaced with 2 mL ASF104 serum-free medium (Ajinomoto, Tokyo, Japan), and the cells were incubated for 72 hours. The medium was then collected, and the cells were washed with phosphate-buffered saline (PBS) and lysed with 2 mL sodium dodecyl sulfate (SDS) sample buffer (62.5 mM Tris (tris(hydroxymethyl) aminomethane)–HCl, 1% SDS, 1% 2-mercaptoethanol, 0.01% bromophenol blue, 5% glycerol, pH 6.8).

Western blot analyses of the expression of ADAMTS-13 mutants

The collected culture media and cell lysates were subjected to 10% SDS–polyacrylamide gel electrophoresis (PAGE) under nonreducing and reducing conditions, respectively, and transferred to an Immobilon polyvinylidene-diflouride membrane (Millipore, Bedford, MA). After blocking with 30% Block Ace (Dainippon Pharmaceutical, Osaka, Japan) in TBST (50 mM Tris-HCl, 100 mM NaCl, and 0.05% Tween 20, pH 7.9) for 1 hour, the membrane was incubated with anti-FLAG M2 monoclonal antibody (MoAb) (Sigma) for 1 hour. After washing, the membrane was incubated with alkaline phosphatase–labeled goat antimouse IgG + M (American Qualex, San Clemente, CA) for 1 hour. The membrane was thoroughly washed with TBST and TBS (50 mM Tris-HCl and 100 mM NaCl, pH 7.9), and labeled bands were visualized with 5-bromo-4-chloro-3-indolyl-phosphate/4-nitroblue tetrazolium chloride (BCIP/NBT; KPL, Gaithersburg, MD).

Assay of VWF-CP activity

VWF was purified from human pooled plasma cryoprecipitate as previously described.[25] VWF-CP activity was detected by using previously reported methods[16,17] with some modifications, as reported previously.[25] Briefly, test samples were preincubated with 10 mM $BaCl_2$ for 5 minutes, and then purified VWF (approximately 200 μg/mL) was mixed with the samples, and the mixtures were dialyzed overnight with the use of a circular dialysis membrane (Millipore) against 5 mM Tris-HCl, pH 8.0, containing 1.5 M urea at 37°C. Subsequently, the reaction mixtures were subjected to SDS-PAGE in a 5% gel under reducing or nonreducing conditions. The gel was stained with Coomassie Brilliant Blue R-250.

Analysis of VWF multimeric pattern

This assay was performed as reported previously.[19] Briefly, 8 μL concentrated culture medium obtained as described in "Transient expression of ADAMTS-13 mutants" was added to 92 μL purified VWF (1 μg) dissolved in reaction buffer (1.5 M urea, 5 mM Tris-HCl, pH 8.0, 10 mM $BaCl_2$, 1 mM phenylmethylsulfonyl fluoride, and 0.05% NaN_3) and incubated at 37°C for 24 hours. After that, 10 μL 100 mM EDTA (ethylenediaminetetraacetic acid, pH 8.0) was added to terminate the reaction. A portion of each reaction mixture was analyzed by SDS–agarose gel electrophoresis, and the multimeric state of VWF was visualized by chemiluminescent Western blot analysis, using anti-VWF antibody.

Purification of inhibitory IgG against ADAMTS-13

IgGs were purified from plasma samples isolated from 3 patients with acquired TTP with the use of a HiTrap protein G HP column (Amersham Biosciences AB, Uppsala, Sweden), according to the manufacturer's instructions. Blood samples were collected from all donors after obtaining informed consent. The inhibitory titers against ADAMTS-13 activity of the 3 plasma samples were 55, 34, and 5.2 Bethesda U/mL. The inhibitor against VWF-CP was measured according to the method by Furlan et al[21] with some modifications.[19] One Bethesda unit of the inhibitor was defined as the amount that reduced ADAMTS-13 activity to 50% compared with an inhibitor negative control. IgG from healthy individuals was used as a control.

Inhibition of VWF-CP activity by inhibitory IgG

Conditioned medium from cells expressing full-length wild-type ADAMTS-13 was preincubated with 10 mM $BaCl_2$ for 5 minutes, and then incubated with an equal volume of purified inhibitory IgG or healthy IgG as negative control for 30 minutes at 37°C. Residual VWF-CP activity of the mixture was performed as described earlier.

Epitope mapping of the inhibitory IgG against ADAMTS-13

Mapping was performed on the basis of Western blot analyses under nonreducing conditions. In practice, 4 membranes containing concentrated (approximately 2- to 20-fold, respectively) culture media of HeLa cells expressing various COOH-terminal truncated ADAMTS-13 mutants were prepared, and each membrane was incubated for 1 hour with anti-FLAG M2 MoAb or 1 of the 3 plasma IgG samples purified as described in "Inhibition of VWF-CP activity by inhibitory IgG." After washing, the membranes were incubated with alkaline phosphatase–labeled goat antihuman IgG

(Rockland, Gilbertsville, PA) for 1 hour. The membranes were washed thoroughly with TBST and TBS, and bound antibody was visualized with BCIP/NBT. Next, to determine the epitope region more precisely, we performed Western blot analysis under nonreducing conditions by using the competitive inhibition method. Briefly, membranes containing the wild-type and the Trp688Xaa mutant proteins were reacted with purified autoantibodies in the absence or presence of a large excess of the concentrated (approximately 10-fold) culture media of HeLa cells expressing full-length wild-type, Trp688Xaa, or Gln449Xaa ADAMTS-13 proteins.

Results

Expression of ADAMTS-13 mutants

To identify essential domains for VWF-CP activity within ADAMTS-13, expression vectors were prepared for 13 sequential COOH-terminally truncated molecules and a single-point mutant (Asp500Glu, ie, RGD to RGE in the cysteine-rich domain), in addition to the full-length wild-type ADAMTS-13 (Figure 1). The FLAG-tag sequence (DYKDDDDK) was added to the COOH-termini of the wild-type and the mutant proteins to assist in immunochemical detection. These plasmids were expressed transiently in HeLa cells. The secretion of each mutant into the culture medium was assessed by Western blot analysis using anti-FLAG M2 antibody (Figure 2A). The immunoreactive bands of truncated mutants ranged from approximately 30 kDa to 200 kDa, corresponding to their expected molecular weights. For the Gly560Xaa, Tyr570Xaa, Thr581Xaa, and Pro590Xaa mutants, however, immunoreactive bands appeared only in the cell lysates and not in the culture media (Figure 2A-B). Shorter truncated mutants, Gln449Xaa, Trp387Xaa, and Pro285Xaa, were secreted into the culture media, indicating that insertion of a stop codon somewhere between the cysteine-rich domain and the spacer domain inhibited normal secretion into the culture medium.

A quantitative assay is required for investigating the relationship between the structure and function in detail. However, expression levels of each mutant and the wild type of ADAMTS-13 were too low to precisely determine the protein concentrations. Furthermore, a variety of molecular forms among all constructs made standardization for a quantitative evaluation difficult. Therefore, the subsequent functional assays were qualitative in nature.

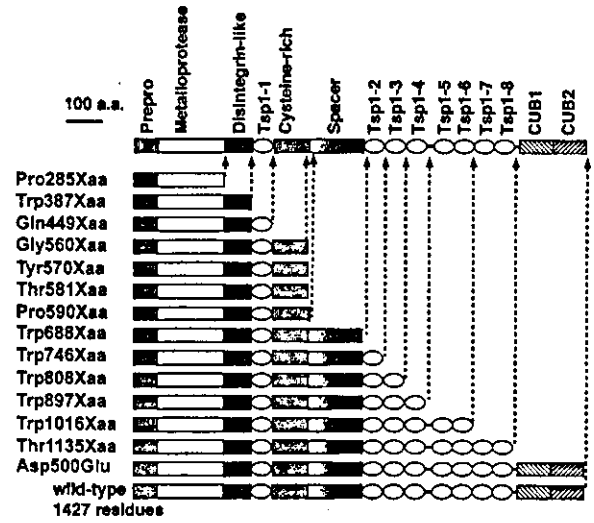

Figure 1. Schematic representation of the domain organization of ADAMTS-13 and construction of mutants. Truncation positions of a series of 13 domain-deleted mutants and the position of a single point mutation (Asp500Glu★) changing a potential cell adhesion motif, RGD, to RGE, are shown.

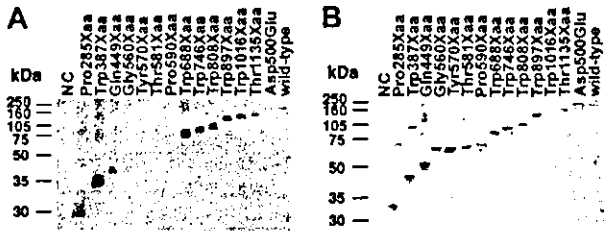

Figure 2. Expression of ADAMTS-13 mutants. HeLa cells were transfected with plasmids encoding FLAG-tagged wild-type or mutant ADAMTS-13. The culture media and cell lysates were analyzed by Western blotting with an anti-FLAG M2 MoAb. (NC) Untransfected culture medium and cell lysate were used as negative controls. (A) Each culture medium sample was subjected to 10% SDS-PAGE under nonreducing conditions. (B) Each cell lysate sample was subjected to 10% SDS-PAGE under reducing conditions.

VWF-CP activity of ADAMTS-13 mutants

VWF-CP cleaves the Tyr842-Met843 bond within VWF, giving rise to 2 fragments with molecular weights of 140 kDa and 176 kDa. VWF-CP activity in the culture medium was measured qualitatively by SDS-PAGE analysis after incubation of VWF with the culture medium. Culture media expressing the Trp688Xaa, Trp746Xaa, Trp808Xaa, Trp897Xaa, Trp1016Xaa, and Thr1135Xaa mutants, as well as the wild-type ADAMTS-13, showed 2 cleaved fragments after incubation with VWF (Figure 3A). The results of NH_2-terminal amino acid sequence analyses of the 176-kDa bands showed that each of these mutant proteins cleaved the Tyr842-Met843 peptide bond within the VWF A2 domain (data not shown). In contrast, it appeared that culture media expressing the Pro285Xaa, Trp387Xaa, and Gln449Xaa mutants, all missing the region from the cysteine-rich domain to the COOH-terminus, showed very low or no activity (Figure 3A), although they were all secreted normally into the culture media (Figure 2A).

Next, the enzyme activities of the wild-type and the mutants were measured by assaying degradation of the VWF multimer. Purified VWF was incubated with the culture medium, and the multimeric state of VWF was determined by Western blot analysis after SDS–agarose electrophoresis (Figure 3B). After the incubation of VWF with the medium of untransfected cells, VWF ladders extended into the high molecular weight area, indicating the absence of VWF-CP activity in the medium (Figure 3B, NC). In contrast, the wild-type culture medium eliminated the high molecular weight bands in the VWF ladder. The deletion mutants devoid of the cysteine-rich and spacer domains had dramatically reduced (Gln449Xaa) or almost negative (Pro285Xaa and Trp387Xaa) levels of this VWF-CP activity. The Trp688Xaa, Trp746Xaa, Trp808Xaa, Trp1016Xaa, and Thr1135Xaa mutants, which contain

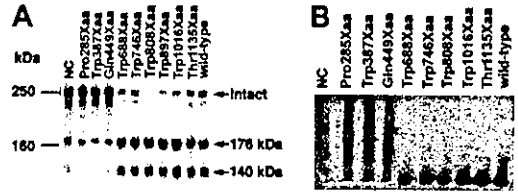

Figure 3. VWF-CP activity of ADAMTS-13 mutants. Culture medium of HeLa cells expressing each mutant was incubated with purified VWF. (A) An aliquot of each reaction mixture was subjected to 5% SDS-PAGE under reducing conditions. The gel was stained with Coomassie Brilliant Blue R-250. (B) An aliquot of each reaction mixture was subjected to SDS–agarose gel electrophoresis. The multimeric patterns of VWF were visualized by Western blot analysis with an anti-VWF antibody.

the cysteine-rich and spacer domains, however, retained their VWF-CP activity (Figure 3B).

The RGD sequence is widely used by proteins for the recognition of integrin, and ADAMTS-13 contains this sequence within the cysteine-rich domain. Therefore, we examined whether the RGD sequence contributes to the enzymatic activity. The VWF-CP activity of the Asp500Glu mutant, in which the RGD sequence was changed to RGE, was measured using the VWF multimer assay (Figure 4). Culture medium from cells expressing the Asp500Glu mutant showed VWF-CP activity equivalent to that of the wild type, indicating that the RGD sequence in ADAMTS-13 is not necessary for VWF multimer degradation under these assay conditions.

Inhibition of VWF-CP activity by 3 patients' IgGs

Three IgG fractions were separately purified from 3 patients with acquired (idiopathic) TTP. The inhibitory potency of these IgGs was assessed as described in "Materials and methods." After overnight incubation of these mixtures with purified VWF, the reaction mixtures were subjected to SDS-PAGE. Cleavage of the Tyr842-Met843 bond within the VWF A2 domain gives rise to 2 fragments with molecular weights of 140 kDa and 176 kDa under reducing conditions, and of approximately 280 kDa and 350 kDa under nonreducing conditions (Figure 5, lanes 4-5). These VWF fragments decreased or disappeared completely in the presence of each patient IgG (Figure 5, lanes 1-3). It was confirmed that these 3 IgG fractions inhibited VWF-CP activity in an in vitro assay system.

Epitope mapping of patient IgG fractions

It is of interest to know the epitopes that these inhibitory IgGs recognize. To characterize such autoantibodies, we performed epitope mapping experiments on the basis of Western blot analyses under nonreducing conditions using 9 deletion mutants truncated from the C-terminus and one missense mutant, Asp500Glu. The 3 purified IgGs were used as the primary antibodies for Western blot analysis. As shown in Figure 6, these IgG fractions preferentially bound to the Trp688Xaa, Trp746Xaa, Trp808Xaa, Trp897Xaa, Trp1016Xaa, Thr1135Xaa, and Asp500Glu mutants as well as to the wild-type protein. The Pro285Xaa, Trp387Xaa, and Gln449Xaa mutants, however, did not react with the autoantibodies at all. Therefore, the major epitopes of the autoantibodies appear to exist somewhere within the cysteine-rich domain to the COOH-terminus.

Subsequently, we performed competitive Western blot analysis to map the epitopes more precisely. Culture media expressing the wild-type and the Trp688Xaa mutant were mixed and subjected to SDS-PAGE for Western blotting under nonreducing conditions. Again, IgG fractions from the 3 patients reacted with the wild-type and the Trp688Xaa mutant, resulting in immunoreactive bands

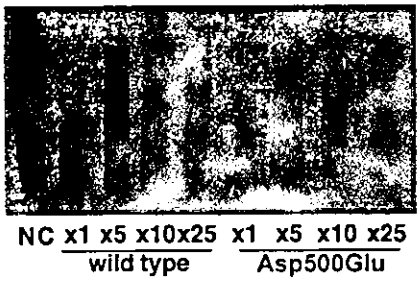

Figure 4. Semiquantitative VWF multimeric state analyses. VWF-CP activity of the wild-type and Asp500Glu mutant proteins was compared. The numbers represent the dilution ratio.

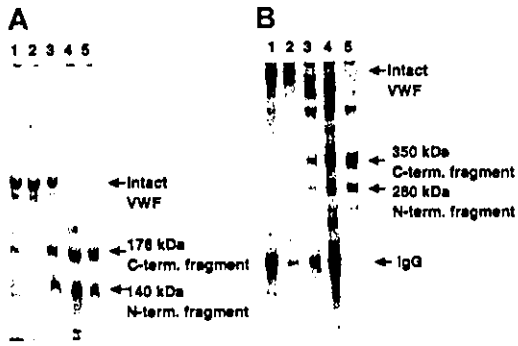

Figure 5. Inhibitory activity of VWF-CP activity of rADAMTS-13 by autoantibodies purified from plasma of patients with acquired TTP. Three IgG fractions were separately purified from 3 patients with acquired (idiopathic) TTP. Preincubated conditioned medium of recombinant wild-type ADAMTS-13 with 10 mM $BaCl_2$ was mixed with an equal volume of purified patient A-C IgGs, (lanes 1-3), healthy IgG (lane 4), or buffer (lane 5), respectively. Then these mixtures were incubated with an equal volume of purified VWF followed by overnight dialysis against 5 mM Tris-HCl, pH 8.0, containing 1.5 M urea at 37°C. An aliquot of each reaction mixture was subjected to 5% SDS-PAGE. The gel was stained with Coomassie Brilliant Blue R-250. (A) Under reducing conditions; (B) under nonreducing conditions.

with molecular masses of approximately 85 kDa (Trp688Xaa) and 210 kDa (wild type), respectively (Figure 7A). Next, the wild-type and the Trp688Xaa mutant proteins on membranes were reacted with purified autoantibodies in the presence of the concentrated culture media of cells expressing Gln449Xaa, Trp688Xaa, or wild-type ADAMTS-13 as competitors for the autoantibodies. The immunopositive bands shown in Figure 7A disappeared completely in the presence of Trp688Xaa or wild-type ADAMTS-13, whereas the addition of Gln449Xaa-containing culture medium caused no effect (Figure 7B). From these results, it is demonstrated that these 3 IgG fractions mainly recognize the region between Trp688Xaa and Gln449Xaa, ie, the cysteine-rich/spacer domains.

Discussion

We summarized all the results obtained in this study in Figure 8. We prepared 13 sequential COOH-terminally truncated molecules and a single point mutant, Asp500Glu, (RGD to RGE in the cysteine-rich domain), and compared the activity of each mutant with that of wild-type recombinant ADAMTS-13 (Figure 1). Deletions located between the cysteine-rich and spacer domains, such as Gly560Xaa, Tyr570Xaa, Thr581Xaa, and Pro590Xaa, abolished secretion into the conditioned medium (Figure 2). These regions might strongly affect the folding and stability of the protein structure. However, truncation mutants lacking the cysteine-rich/spacer domains, including Gln449Xaa, Trp387Xaa, and Pro285Xaa, exhibited dramatically reduced or almost negative VWF-CP activity (Figure 3). These results were similar to those demonstrated by Zheng et al.[36]

On the other hand, Schneppenheim et al[37] demonstrated that patients with TTP, with truncation in ADAMTS-13 downstream of the cysteine-rich/spacer domain, such as Arg910Xaa and Arg1034Xaa, suffered from severe deficiency of VWF-CP activity, in that ADAMTS-13 mutants were truncated within the C-terminal Tsp1 motif repeats. However, it is speculated that these truncated forms may not have the ability to form disulfide bonds because a stop codon is inserted within an intradomain of a Tsp1 motif. Therefore, these mutants appear to be very unstable, resulting in the abnormality of secretion. In contrast, the truncated forms we constructed, such as Trp897Xaa, Trp1016Xaa, and Thr1135Xaa,

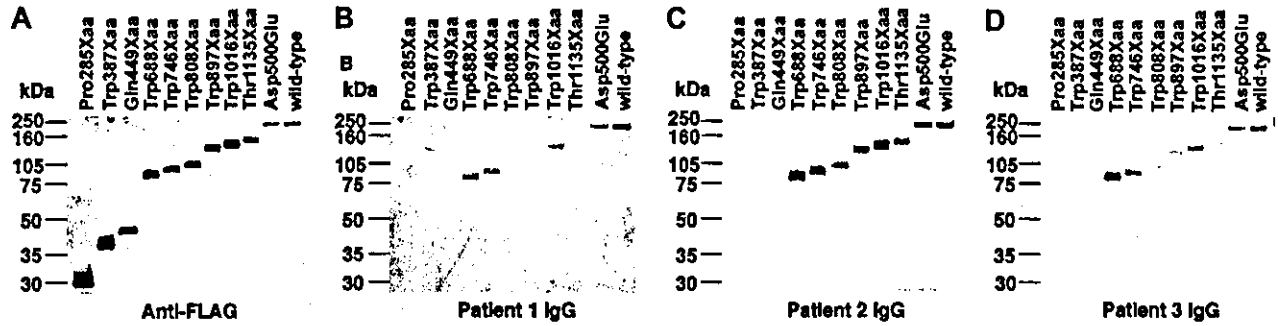

Figure 6. Epitope mapping of anti-ADAMTS-13 autoantibodies in patients with acquired TTP. The culture media of various COOH-terminally truncated mutants were blotted onto polyvinylidene difluoride membranes. The membranes were reacted with anti-FLAG M2 MoAb as a positive control (A) or anti–ADAMTS-13 inhibitory autoantibodies from 3 patients with acquired TTP (B-D).

were secreted normally and retained VWF-CP activity, because a stop codon is inserted between domains.

Moreover, we prepared an active site mutated protein, Glu225Ala, which replaced Glu to Ala within the zinc-binding motif (HEXXHXXGXXHD) of metalloprotease domain, to confirm that this domain is responsible for VWF cleavage. As expected, mutation of a critical residue in the active center within the metalloprotease domain, Glu225Ala, caused a loss in activity (data not shown). From these results, we conclude that protease domain to cysteine-rich/spacer domains are indispensable regions for expressing VWF-CP activity under the assay conditions described here.

Binding sites for sulfated glycosaminoglycans are known to exist within the spacer domain of ADAMTS-1 (METH-1).[38] According to a previous report on ADAMTS-4 (Aggrecanase-1), binding sites for sulfated glycosaminoglycans attached to the aggrecan core protein are located within the ADAMTS-4 cysteine-rich/spacer domains.[39] Furthermore, analyses of chimeras encoding domains of *Xenopus* ADAMs 10 and 13 suggested that ADAM-13 metalloprotease might use its cysteine-rich domain to improve its specificity or activity in cleaving a substrate(s).[40] In addition, the ADAMTS-13 cysteine-rich domain contains one RGD motif, a potential cell adhesion sequence, although the sequence is not required for the expression of VWF-CP activity in the assay conditions as described in "Materials and methods" (Figure 4). On the basis of these findings, it seems possible that the ADAMTS-13 cysteine-rich/spacer domains function as a cell surface receptor binding site and/or substrate recognition exosite.

Results on Western blot analyses demonstrated that the major epitope of IgGs separated from plasma of 3 patients with acquired TTP possessing inhibitory activity against VWF-CP (Figure 5) was located within cysteine-rich/spacer domains (Figures 6-7). Therefore, it seems reasonable that these IgGs bind to cysteine-rich/spacer domains, resulting in the inhibition of VWF-CP activity. From these results, it is likely that the ADAMTS-13 cysteine-rich/spacer domains are involved in VWF recognition.

It was also speculated that anchorage of ADAMTS-13 on the endothelial cell surface via additional COOH-terminal Tsp1 repeats is necessary for expression of VWF-CP activity in vivo.[31] By considering that finding together with our present results, ADAMTS-13 on the endothelial cell surface may interact with VWF through the cysteine-rich/spacer domains and cleave it via the metalloprotease domain in vivo.

The present study clearly demonstrates that ADAMTS-13 cysteine-rich/spacer domains are functionally essential for VWF cleavage; however, it is impossible to deny the theoretical possibility that the results in the present study could be explained by an indirect effect on folding as a result of the deletion of the cysteine-rich/spacer domains. Furthermore, on the epitope mapping experiment using polyclonal autoantibodies, possibilities of a complex conformational epitope involving other N-terminal segments or of contamination of a trace amount of antibodies against other domain(s), for example metalloprotease domain, cannot be excluded. In the future, these possibilities might be examined by the analysis of a complementary set of N-terminal deletions and/or by an experiment using specific antibody against cysteine-rich/spacer domains. Moreover, further studies may reveal that the critical segment is restricted to just the small remaining stretch of cysteine-rich domain or within just the spacer domain, and that one or the other segment is not required.

Figure 7. Precise epitope mapping of IgG fractions from patients with acquired TTP by competitive immunoblot analysis. Two culture medium samples, one from cells transfected with the full-length wild-type plasmid and the other from cells transfected with the Trp688Xaa plasmid, were premixed, subjected to SDS-PAGE, and blotted onto polyvinylidene difluoride membranes. (A) Each blot was reacted with healthy IgG, anti-FLAG M2 MoAb, or IgGs prepared from 3 patients. (B) Each blot was reacted with IgGs prepared from 3 patients in the presence of 10-fold concentrated cultured media of cells transfected with either the Gln449Xaa, the Trp688Xaa, or the full-length wild-type plasmid.

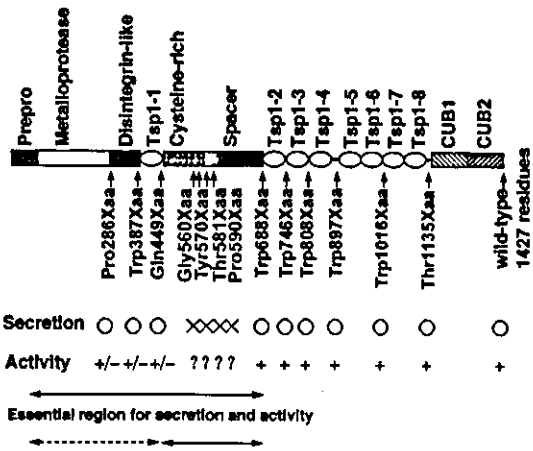

Figure 8. Schematic representation of the functionally important region of ADAMTS-13. O indicates normal secretion; ×, no secretion. +, VWF-CP activity is positive; ?, no test; +/−, very low or no activity.

Acknowledgments

We thank Prof Emeritus Sadaaki Iwanaga (Kyushu University) for his critical reading of the manuscript, as well as Drs Shouichi Higashi (Yokohama City University), Jun Mizuguchi, Shintaro Kamei, and Tsutomu Hamuro (The Chemo-Sero-Therapeutic Research Institute) for many helpful suggestions. We also thank Noriko Mimura and Masaki Hirashima (The Chemo-Sero-Therapeutic Research Institute) for their technical support.

References

1. Zimmerman TS, Ruggeri ZM. von Willebrand disease. Hum Pathol. 1987;18:140-152.
2. Jaffe EA, Hoyer LW, Nachman RL. Synthesis of von Willebrand factor by cultured human endothelial cells. Proc Natl Acad Sci U S A. 1974;71: 1906-1909.
3. Fujimura Y, Titani K. Structure and function of von Willebrand factor. In: Bloom AL, Forbes CD, Thomas DP, Tuddenham EGD, eds. Haemostasis and Thrombosis. New York, NY: Churchill Livingstone; 1994:379-395.
4. Ruggeri ZM. von Willebrand factor. J Clin Invest. 1997;99:559-564.
5. Sadler JE. Biochemistry and genetics of von Willebrand factor. Annu Rev Biochem. 1998;67:395-424.
6. Ruggeri ZM, Zimmerman TS. The complex multimeric composition of factor VIII/von Willebrand factor. Blood. 1981;57:1140-1143.
7. Sixma JJ, Sakariassen KS, Beeser-Visser NH, Ottenhof-Rovers M, Bolhuis PA. Adhesion of platelets to human artery subendothelium: effect of factor VIII-von Willebrand factor of various multimeric composition. Blood. 1984;63:128-139.
8. Sporn LA, Marder VJ, Wagner DD. von Willebrand factor released from Weibel-Palade bodies binds more avidly to extracellular matrix than that secreted constitutively. Blood. 1987;69:1531-1534.
9. Zimmerman TS, Dent JA, Ruggeri ZM, Nannini LH. Subunit composition of plasma von Willebrand factor: cleavage is present in normal individuals, increased in IIA and IIB von Willebrand disease, but minimal in variants with aberrant structure of individual oligomers (types IIC, IID, and IIE). J Clin Invest. 1986;77:947-951.
10. Berkowitz SD, Dent J, Roberts J, et al. Epitope mapping of the von Willebrand factor subunit distinguishes fragments present in normal and type IIA von Willebrand disease from those generated by plasmin. J Clin Invest. 1987;79:524-531.
11. Dent JA, Galbusera M, Ruggeri ZM. Heterogeneity of plasma von Willebrand factor multimers resulting from proteolysis of the constituent subunit. J Clin Invest. 1991;88:774-782.
12. Furlan M, Robles R, Affolter D, Meyer D, Baillod P, Lämmle B. Triplet structure of von Willebrand factor reflects proteolytic degradation of high molecular weight multimers. Proc Natl Acad Sci U S A. 1993;90:7503-7507.
13. Dent JA, Berkowitz SD, Ware J, Kasper CK, Ruggeri ZM. Identification of a cleavage site directing the immunochemical detection of molecular abnormalities in type IIA von Willebrand factor. Proc Natl Acad Sci U S A. 1990;87:6306-6310.
14. Moake JL, Rudy CK, Troll JH, et al. Unusually large plasma factor VIII:von Willebrand factor multimers in chronic relapsing thrombotic thrombocytopenic purpura. N Engl J Med. 1982;307: 1432-1435.
15. Moschcowitz E. Hyalin thrombosis of the terminal arterioles and capillaries: a hitherto undescribed disease. Proc N Y Pathol Soc. 1924;24:21-24.
16. Furlan M, Robles R, Lämmle B. Partial purification and characterization of a protease from human plasma cleaving von Willebrand factor to fragments produced by in vivo proteolysis. Blood. 1996;87:4223-4234.
17. Tsai H-M. Physiologic cleavage of von Willebrand factor by a plasma protease is dependent on its conformation and requires calcium ion. Blood. 1996;87:4235-4244.
18. Furlan M, Robles R, Solenthaler M, Wassmer M, Sandoz P, Lämmle B. Deficient activity of von Willebrand factor-cleaving protease in chronic relapsing thrombotic thrombocytopenic purpura. Blood. 1997;89:3097-3103.
19. Kinoshita S, Yoshioka A, Park YD, et al. Upshaw-Schulman syndrome revisited: a concept of congenital thrombotic thrombocytopenic purpura. Int J Hematol. 2001;74:101-108.
20. Furlan M, Robles R, Galbusera M, et al. von Willebrand factor-cleaving protease in thrombotic thrombocytopenic purpura and the hemolytic-uremic syndrome. N Engl J Med. 1998;339:1578-1584.
21. Furlan M, Robles R, Solenthaler M, Lämmle B. Acquired deficiency of von Willebrand factor-cleaving protease in a patient with thrombotic thrombocytopenic purpura. Blood. 1998;91:2839-2846.
22. Tsai H-M, Lian EC. Antibodies to von Willebrand factor-cleaving protease in acute thrombotic thrombocytopenic purpura. N Engl J Med. 1998; 339:1585-1594.
23. Gerritsen HE, Robles R, Lämmle B, Furlan M. Partial amino acid sequence of purified von Willebrand factor-cleaving protease. Blood. 2001;98: 1654-1661.
24. Fujikawa K, Suzuki H, McMullen B, Chung D. Purification of human von Willebrand factor-cleaving protease and its identification as a new member of the metalloproteinase family. Blood. 2001;98: 1662-1666.
25. Soejima K, Mimura N, Hirashima M, et al. A novel human metalloprotease synthesized in the liver and secreted into the blood: possibly, the von Willebrand factor-cleaving protease? J Biochem (Tokyo). 2001;130:475-480.
26. Zheng X, Chung D, Takayama TK, Majerus EM, Sadler JE, Fujikawa K. Structure of von Willebrand factor-cleaving protease (ADAMTS13), a metalloprotease involved in thrombotic thrombocytopenic purpura. J Biol Chem. 2001;276: 41059-41063.
27. Levy GG, Nichols WC, Lian EC, et al. Mutations in a member of the ADAMTS gene family cause thrombotic thrombocytopenic purpura. Nature. 2001;413:488-494.
28. Cal S, Obaya AJ, Llamazares M, Garabaya C, Quesada V, Lopez-Otin C. Cloning, expression analysis, and structural characterization of seven novel human ADAMTSs, a family of metalloproteinases with disintegrin and thrombospondin-1 domains. Gene. 2002;283:49-62.
29. Plaimauer B, Zimmermann K, Volkel D, et al. Cloning, expression, and functional characterization of the von Willebrand factor-cleaving protease (ADAMTS13). Blood. 2002;100:3626-3632.
30. Matsumoto M, Chisuwa H, Nakazawa Y, et al. Living-related liver transplantation rescues reduced vWF-cleaving protease activity in patients with cirrhotic biliary atresia [abstract]. Blood. 2000;96:636a.
31. Dong JF, Moake JL, Nolasco L, et al. ADAMTS-13 rapidly cleaves newly secreted ultralarge von Willebrand factor multimers on the endothelial surface under flowing conditions. Blood. 2002;100:4033-4039.
32. Ruoslahti E, Pierschbacher MD. Arg-Gly-Asp: a versatile cell recognition signal. Cell. 1986;44: 517-518.
33. Kokame K, Matsumoto M, Soejima K, et al. Mutations and common polymorphisms in ADAMTS13 gene responsible for von Willebrand factor-cleaving protease activity. Proc Nat Acad Sci U S A. 2002;99:11902-11907.
34. Niwa H, Yamamura K, Miyazaki J. Efficient selection for high-expression transfectants with a novel eukaryotic vector. Gene. 1991;108:193-199.
35. Soejima K, Mizuguchi J, Yuguchi M, Nakagaki T, Higashi S, Iwanaga S. Factor VIIa modified in the 170 loop shows enhanced catalytic activity but does not change the zymogen-like property. J Biol Chem. 2001;276:17229-17235.
36. Zheng X, Nishio K, Majerus E, Sadler JE. Characterization of recombinant ADAMTS-13 in COS7 cells and identification of domains required for cleavage of von Willebrand factor [abstract]. Blood. 2002;100:256a.
37. Schneppenheim R, Budde U, Oyen F, et al. Von Willebrand factor cleaving protease and ADAMTS13 mutations in childhood TTP. Blood. 2003;101:1845-1850.
38. Kuno K, Matsushima K. ADAMTS-1 protein anchors at the extracellular matrix through the thrombospondin type I motifs and its spacing region. J Biol Chem. 1998;273:13912-13917.
39. Flannery CR, Zeng W, Corcoran C, et al. Autocatalytic cleavage of ADAMTS-4 (Aggrecanase-1) reveals multiple glycosaminoglycan-binding sites. J Biol Chem. 2002;277:42775-42780.
40. Smith KM, Gaultier A, Cousin H, Alfandari D, White JM, DeSimone DW. The cysteine-rich domain regulates ADAM protease function in vivo. J Cell Biol. 2002;159:893-902.

Journal of Thrombosis and Haemostasis, 1: 2397–2403

ORIGINAL ARTICLE

Population-based distribution of plasminogen activity and estimated prevalence and relevance to thrombotic diseases of plasminogen deficiency in the Japanese: the Suita Study

A. OKAMOTO,* T. SAKATA,* T. MANNAMI,† S. BABA,†[1] Y. KATAYAMA,* H. MATSUO,†[2] M. YASAKA,§ K. MINEMATSU,§ H. TOMOIKE† and T. MIYATA*

*Laboratory of Clinical Chemistry, Departments of †Preventive Cardiology, and ‡Cardiology, §Cerebrovascular Division, Department of Medicine, *Research Institute, National Cardiovascular Center, Osaka, Japan*

To cite this article: Okamoto A, Sakata T, Mannami T, Baba S, Katayama Y, Matsuo H, Yasaka M, Minematsu K, Tomoike H, Miyata T. Population-based distribution of plasminogen activity and estimated prevalence and relevance to thrombotic diseases of plasminogen deficiency in the Japanese: the Suita Study. *J Thromb Haemost* 2003; 1: 2397–403.

Summary. Reduced plasminogen activity with a normal level of antigen is commonly observed in Japanese individuals. The first reported patient with plasminogen deficiency was accompanied with deep vein thrombosis. The present study examines whether heterozygous or homozygous deficiency of plasminogen is a risk factor for thrombotic disease. This study measures the plasminogen activity of 4517 individuals in the general population, determines the cut-off to define plasminogen deficiency, and identifies plasminogen deficiencies in the control groups and thrombotic disease groups. In another study, we examined the phenotypes of consecutive patients with homozygous plasminogen deficiency detected in our hospital. We found 173 and two of 4517 individuals to have heterozygous and homozygous deficiency with normal plasminogen antigen level, respectively, and 19 to have heterozygous deficiency with reduced antigen levels. The incidence of plasminogen deficiency in an age- and sex-matched control group (13/324, 4.01% for deep vein thrombosis or 13/330, 3.94% for stroke) selected from the 4517 individuals was not significantly different from those in patients with deep vein thrombosis (3/108, 2.78%) or cardioembolic stroke (6/110, 5.55%). Among 19 patients with homozygous plasminogen deficiency showing about 10% plasminogen activity, none had deep vein thrombosis. These findings indicate that neither heterozygous nor homozygous plasminogen deficiency constitutes a significant risk factor for thrombotic disease.

Keywords: deep vein thrombosis, genetic variant, plasminogen deficiency, risk factor.

Plasminogen deficiency is classified into two groups; one is type I deficiency characterized by the parallel reduction of both activity and antigen and the other is dysplasminogenemia (type II), characterized by reduced activity with a normal antigen level [1].

In 1978, a Japanese patient with recurrent vein thrombosis was found to have a hereditary molecular defect of plasminogen [2]. The patient showed low activity of plasminogen but the antigen level was within normal limits, indicating type II deficiency [2,3]. The molecular defect of this mutant plasminogen, referred to as plasminogen Tochigi, was a G→A transition mutation leading to an Ala→Thr substitution at position 601 near the active site triad [4,5].

A few small studies estimated the frequency of plasminogen deficiency in Japanese and reported the allele frequency of plasminogen Tochigi mutation to be between 1.1 and 2.1% [6–9]. It is now known that over 94% of plasminogen deficiency in the Japanese population is attributable to plasminogen Tochigi [10]. The mutation also was found in the Chinese Han population with an allele frequency of 1.4–1.5% [9,11] and in the Korean population with an allele frequency of 1.6% [9]. A homozygous patient with plasminogen Tochigi has also been reported; the plasminogen showed very low but significant activity [3], and this finding was supported by the molecular model of the plasmin mutant [12]. On the other hand, type I plasminogen deficiency has been detected in isolated families [13–16]. Recently, type I plasminogen deficiency has been reported to be associated with ligneous conjunctivitis, a rare form of chronic conjunctivitis characterized by chronic tearing and redness of the conjunctivas [15,16].

Correspondence: Toshiyuki Sakata, Laboratory of Clinical Chemistry, National Cardiovascular Center, 5-7-1 Fujishirodai, Suita, Osaka 565–8565, Japan.
Tel.: +81 6 68335012 (ext. 2296); fax: +81 6 68351176; e-mail: tsakata@hsp.ncvc.go.jp

[1]Present address: Shunroku Baba, The Second Hanwa Hospital, 3176 Fukaikitamachi, Sakai-City, Osaka, 599-8271, Japan.
[2]Present address: Hiroshi Matsuo, Matsuo Cardiovascular Clinic, Nichiei Bldg., 1-4-8 Tosabori, Nishi-ku, Osaka, 550–0001, Japan.

Received 30 October 2002, accepted 28 May 2003

The first report [2] linking plasminogen deficiency to thrombosis was followed by many similar publications [13–16]. However, some recent studies did not support the link [17–19]. Among 1192 consecutive patients with a history of venous and/or arterial thrombosis, plasminogen deficiency was not a risk factor for thrombosis [17]. A large cohort study performed in Scotland also denied the link. That study identified 28 individuals with plasminogen deficiency out of 9611 donors, with a prevalence of 0.29% [18], which was not significantly different from the prevalence (0.54%) calculated from studies of thrombotic cohorts in the literature, indicating that plasminogen deficiency is not a risk factor for thrombosis. However, these studies had some limitations such as comparison of frequencies obtained among populations with geographic distance.

We conducted an epidemiological study of plasminogen deficiency in over 4500 Japanese in the general population. We also measured the plasminogen activity in patient groups with thrombotic complications, most of whom reside in the same area where the epidemiological study was performed.

Materials and methods

Study population for control group

The population for the reference group was based on a random sample selected from the residents of Suita, a city located in the second largest urban area in Japan (Osaka area). The sample comprised 12 200 men and women aged 32–89 years. The basic sampling of the population started in 1989 with a cohort study base [20–22]. The subjects have been visiting the National Cardiovascular Center every 2 years since then for regular health check-ups. In addition to performing a routine blood examination that included total serum cholesterol, HDL cholesterol, triglyceride, and glucose levels and blood pressure and anthropometric measurements, a physician or nurse administered questionnaires covering personal history of cardiovascular diseases, including angina pectoris, myocardial infarction (MI), and/or stroke.

The subjects for the reference group included 4526 blood donors who attended regular health checkups between August 1998 and July 2000. The subjects were only those who agreed to have a blood examination. Eight samples not properly harvested (e.g. hemolyzed blood, incorrect sample volume) were not included. An individual taking anticancer drugs ($n = 1$) was also excluded. Finally, 4517 blood donors (2090 men, 2427 women) were enrolled for measurement of plasminogen activity. Age-matched and sex-matched controls ($n = 324$ and $n = 330$, respectively) for deep vein thrombosis (DVT) and for cardioembolic stroke due to non-valvular atrial fibrillation (NVAF) were selected from among the subjects without cardiovascular diseases.

Patients groups

Between April 1994 and March 1998, 108 consecutive outpatients (54 men, 54 women; mean age ± SD, 57.8 ± 17.2 years, 49.6 ± 18.0 years, respectively) with DVT admitted to the Department of Cardiology of National Cardiovascular Center were enrolled. The diagnoses of DVT were based on radioisotope venography and/or contrast venography. As another patient group, we enrolled 110 patients (77 men, 33 women; mean age ± SD, 66.8 ± 9.6 years, 64.7 ± 11.8 years, respectively) with NVAF at the outpatient clinic of the Cerebrovascular Division of the National Cardiovascular Center in July and August of 1998, who had been diagnosed as cardioembolic stroke according to the criteria previously mentioned more than one month prior to the enrollment [23]. All of them had received warfarin therapy against recurrence of cardioembolic stroke.

Concerning homozygous plasminogen deficiency, we screened for plasminogen activity in patients admitted to our hospital from 1992 to 2000 and identified 19 patients with homozygous plasminogen deficiency. All of the patients were followed for several years to measure their plasminogen activity and again showed very low activities more than twice. Five patients out of 19 were confirmed by the family study (more than one of their family members showed low plasminogen activity [heterozygous deficiency]). We simultaneously measured prothrombin time and activated partial prothrombin time and the plasma levels of antithrombin, protein C, α_2-plasmin inhibitor, and fibrin degradation products in these patients to exclude the possibility of activation of blood coagulation or fibrinolysis system.

Sample collection and analysis

We obtained blood samples before noon after an overnight fast. Blood samples were collected in siliconized vacuum plastic tubes containing 1/10 volume of 3.13% trisodium citrate. Tubes were centrifuged at 3600 × *g* for 10 min at room temperature. After separation, if analysis was not to be performed immediately, the plasma samples were frozen at −80 °C for storage until laboratory determinations were performed.

Plasminogen activity was measured by the chromogenic assay method using streptokinase as the activator and the specific substrate S-2251 (Chromogenix AB, Stockholm, Sweden). Plasminogen antigen was measured by the turbidimetric immunoassay method using antiserum to human plasminogen (Behringwerke, Marburg, Germany). Antithrombin activity was measured as a heparin cofactor activity by use of the chromogenic substrate S-2238 (Chromogenix AB). The plasma levels of plasminogen and antithrombin were expressed as percentages of the levels obtained from commercially available standard human plasma (Behringwerke). As measured in our laboratory, the interassay coefficients of variation were 2.0% for the plasminogen activity assay, 3.5% for the plasminogen antigen assay and 2.2% for the antithrombin assay.

Statistical analysis

Spearman correlation analysis was used to assess the association between aging and the level of plasminogen activity and was performed by gender. Plasminogen activity in the 10-year

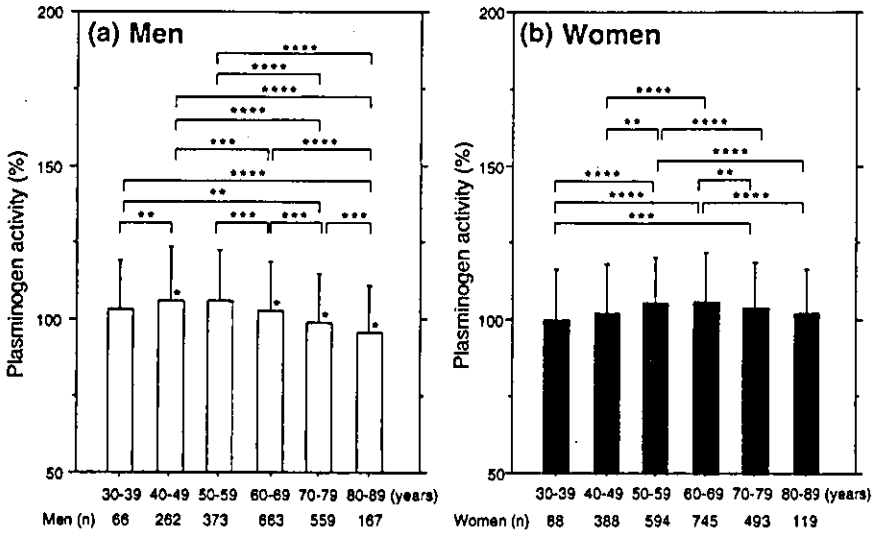

Fig. 1. Age- and sex-related changes in plasminogen activity in the Japanese general population ($n = 4517$). Open and closed bars show the plasminogen activities in men (a) and women (b), respectively. $^{*}P < 0.001$, compared with those in women of the same age group. $^{**}P < 0.05$, $^{***}P < 0.01$, $^{****}P < 0.001$, compared with those in other age groups within the same sex.

age groups in men and women was recorded as mean ± SD. As the data did not show a Gaussian distribution in Fig. 1, we chose the non-parametric Kruskal–Wallis test for comparison among multiple groups. For comparison between two groups, the Mann–Whitney *U*-test was used. Odds ratios with corresponding 95% confidence intervals were used to assess the differences between prevalence rates from different populations. Differences with a value of $P < 0.01$ for the Spearman correlation analysis and $P < 0.05$ for the Kruskal–Wallis test, the Mann–Whitney *U*-test and odds ratios were considered to be significant. Statistical calculations were performed using SPSS version 10.0 (SPSS Inc, Chicago, IL, USA).

Results

Age- and sex-related changes and distribution of plasminogen activity

We measured the activities of plasminogen and antithrombin in 4517 individuals who participated in the Suita Study. The mean ± SD of plasminogen activity in all donors, men and women, was 103.6 ± 15.9 (mean ± 2 SD range; 72–135%), 102.4 ± 16.4 (mean ± 2 SD range; 70–135%), and 104.6 ± 15.3 (mean ± 2 SD range; 74–135%), respectively. Figure 1 shows the age-related distribution (32–89 years) of plasminogen activity in 2090 men (Fig. 1a) and 2427 women (Fig. 1b). As a whole, a linear decrease of plasminogen activity with age was observed in men ($r = -0.24$, $P < 0.0001$), but not in women ($r = 0.02$, $P = 0.36$). When the activity was analyzed in 10-year age groups, a slight increase was observed in the men aged 30–39 years and 40–49 years ($P < 0.05$) and in the women aged 30–39 years and 50–59 years ($P < 0.001$). The levels of plasminogen activity were decreased in both sexes in the elder age groups. As a gender-related change, the level of plasminogen in the age group of 40–49 years in men was significantly higher than that in women. In contrast, the levels in women in the age groups of 60–69, 70–79, and 80–89 years were significantly higher than those in men.

Identification of plasminogen deficiency

Figure 2(a) shows the distribution of the plasminogen activity in 4517 individuals. The plasminogen activity showed one big peak in the number of subjects and a small and broad peak at around 60% plasminogen activity, which consisted of the subjects with plasminogen deficiency. It was hard to distinguish whether an individual who showed marginal activity was plasminogen deficient or not. In identification of protein C deficiency, the ratio of protein C and factor X was recommended for the identification of the deficient by the Scientific

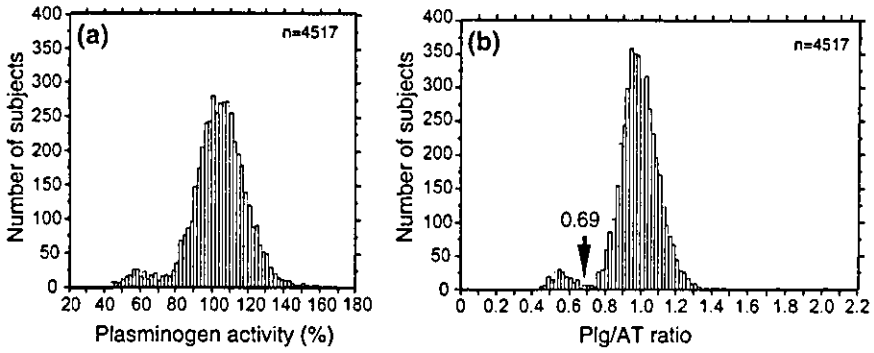

Fig. 2. Distribution of plasminogen activity and plasminogen/antithrombin ratio in the 4517 cohort. Each histogram bar shows the numbers of subjects in every 2% of plasminogen activity (a) or in every 0.02 of the plasminogen/antithrombin activity (Plg/AT) ratio (b). The arrow indicates the cut-off in the plasminogen/antithrombin ratio, 0.69.

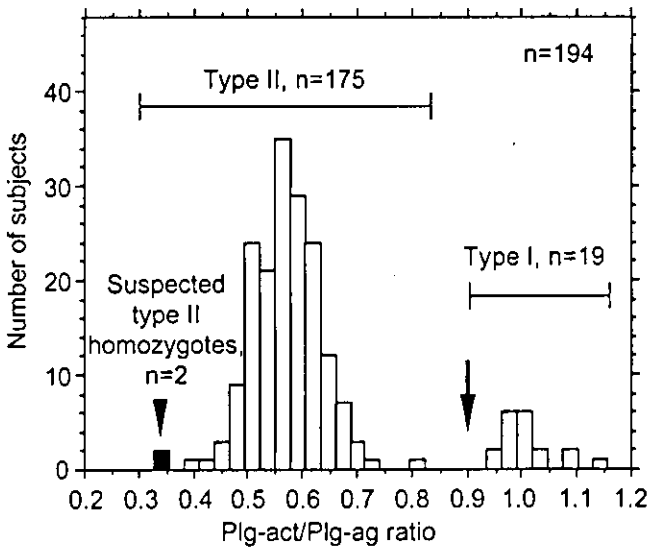

Fig. 3. Distribution of activity/antigen ratio of plasminogen (Plg-act/Plg-ag) in 194 individuals with plasminogen deficiency. The arrow indicates the cut-off point, 0.9. Nineteen individuals showed ratios over 0.9, indicating type I plasminogen deficiency, and 175 individuals showed ratios less than 0.9, indicating type II plasminogen deficiency. Among type II deficiency, two showed very low ratios indicating homozygous type II deficiency.

and Standardization Committee of the International Society on Thrombosis and Haemostasis [24]. In our study, we calculated the ratio of plasminogen activity to antithrombin activity (Fig. 2b). As a result, the two peaks were clearly separated. The mean −2 SD of the ratio was 0.69. To distinguish the plasminogen deficiency from the normal plasminogen, we used the ratio 0.69 as the cut-off. Only 192 among 4517 showed ratios less than 0.69.

Of the individuals with ratios higher than 0.69, two showed low plasminogen and antithrombin activities with normal levels of plasminogen antigen and protein C, indicating a combined deficiency of plasminogen and antithrombin (subject 1: male, age 70 years, plasminogen activity 59.4%, plasminogen antigen 110.6%, antithrombin activity 65.8%, protein C 110.8%; subject 2: male, age 75 years, plasminogen activity 69.8%, plasminogen antigen 118.0%, antithrombin activity 74.2%, protein C 123.8%). Thus, a total of 194 individuals (194/4517, 4.30%) were considered to be plasminogen-deficient. Among 194 individuals, two showed extremely low plasminogen activity, indicating a homozygous plasminogen deficiency (subject 3: male, age 60 years, plasminogen activity 24.4%, plasminogen antigen 74.0%, antithrombin activity 97.2%, protein C 120.1%; subject 4: male, age 80 years, plasminogen activity 26.2%, plasminogen antigen 78.4%, antithrombin activity 67.2%, protein C 61.3%).

Plasminogen deficiency (194 individuals) can be divided into two groups, type I (hypoplasminogenemia) or type II (dysplasminogenemia), and can be judged by the ratio of activity and antigen of plasminogen (Plg-act/Plg-ag). Figure 3 shows the distribution of the Plg-act/Plg-ag ratio. The Plg-act/Plg-ag ratio exhibited two peaks. We set the cut-off of the ratio to be 0.90. Nineteen out of 194 individuals were classified into type I plasminogen deficiency, and the remaining 175 were type II plasminogen deficiency, including two suspected homozygous plasminogen deficiency.

Consequently, in the Japanese general population, the overall prevalence of heterozygous type I plasminogen deficiency was 0.42% ($n = 19$; men $n = 8$; women $n = 11$) and heterozygous and homozygous type II plasminogen deficiency were 3.83% ($n = 173$; men $n = 82$; women $n = 91$) and 0.04% ($n = 2$; men $n = 2$; women $n = 0$), respectively (Fig. 4).

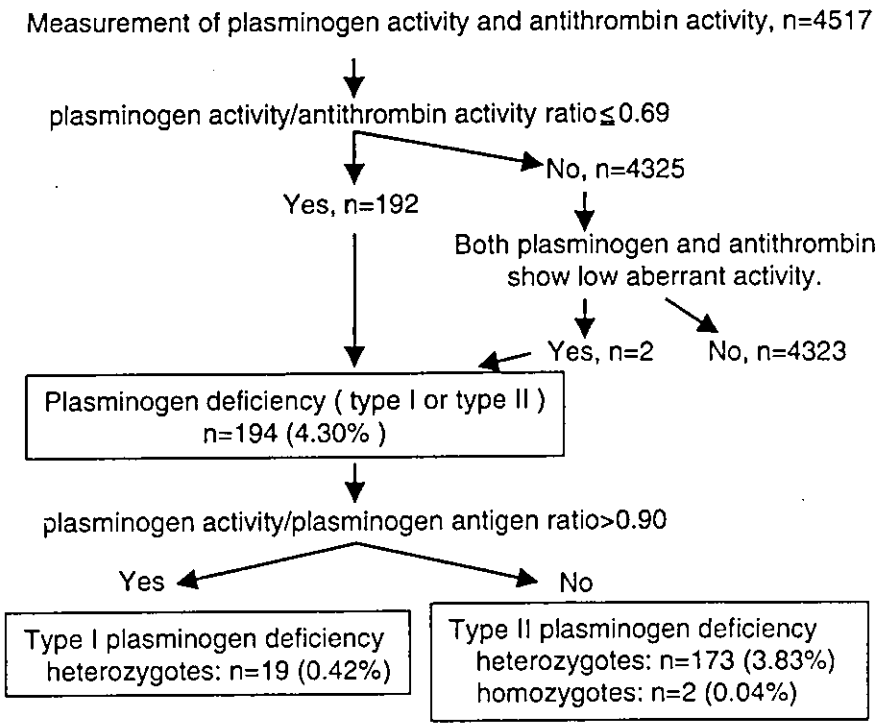

Fig. 4. Flow chart of selection of individuals with plasminogen deficiency. To identify the plasminogen deficiency in 4715 individuals, we performed a two-stage selection. The first used a 0.69 plasminogen/antithrombin ratio as the cut-off to distinguish the deficients from the normals, and the second used a 0.9 activity/antigen ratio of plasminogen for discrimination of plasminogen deficiency type I and type II.